

Search for new physics in the 2011 opposite sign dilepton sample

D. Barge, C. Campagnari, P. Kalavase, D. Kovalskyi, V. Krutelyov, J. Ribnik

University of California, Santa Barbara

W. Andrews, G. Cerati, D. Evans, F. Golf, I. Macneill, S. Padhi, Y. Tu, F. Würthwein, A. Yagil, J. Yoo

University of California, San Diego

L. Bauerdick, I. Bloch, K. Burkett, I. Fisk, Y. Gao, O. Gutsche, B. Hooberman, S. Jindariani

Fermi National Accelerator Laboratory, Batavia, Illinois

Version v0

Abstract

We present the results of a search for new physics in the opposite-sign leptons + jets + missing energy final state based on 204 pb^{-1} of 2011 CMS data.

Contents

1	Introduction	2
2	Datasets, Triggers, Luminosity	2
3	Event Preselection	3
3.1	Event Cleanup	3
3.2	Muon Selection	3
3.3	Electron Selection	4
3.4	Invariant mass requirement	4
3.5	Trigger Selection	4
4	Trigger efficiency	5
5	Dilepton Yields	5
6	Preselection yields	6
7	Properties of data passing the preselection	7
8	Definition of the signal region	7
9	Data Driven Background Estimation Methods	10
9.1	ABCD method	11
9.2	Dilepton P_T method	13
9.3	Opposite-Flavor Subtraction	14
9.3.1	OF subtraction: Application to high p_T lepton sample	14
9.3.2	OF subtraction: Application to low p_T lepton sample	14
10	Results	14
10.1	Background estimate from the ABCD method	14
10.2	Background estimate from the $P_T(\ell\ell)$ method	18
10.3	Background estimate from OF subtraction	18
10.4	Summary of results	18
	Appendix A Fakeable Object Definitions	21
	Appendix B The ABCD' Method	21
	Appendix C Data/MC Comparison: Preselection Region	21
	Appendix D Data/MC Comparison: 2010 Signal Region	42

1 Introduction

In this note we describe a search for new physics in the 2011 opposite sign isolated dilepton sample (ee , $e\mu$, and $\mu\mu$) based on 204 pb^{-1} . The main source of isolated dileptons at CMS is Drell Yan and $t\bar{t}$. Here we concentrate on dileptons with invariant mass inconsistent with $Z \rightarrow ee$ and $Z \rightarrow \mu\mu$, thus $t\bar{t}$ is the most important background. A separate search for new physics in the Z sample is described in a separate note [1]. This is an update of a (soon to be) published analysis performed on 2010 data [2, 3].

The search strategy is the following

- We start out with a pre-selection which is as close as possible to the published $t\bar{t}$ dilepton analysis [4] (same lepton ID, same jet definitions, etc.). We do make a couple of substantive modifications:
 1. The top analysis requires two leptons of $p_T > 20 \text{ GeV}$. In this analysis we search for new physics in 2 data samples. The first data sample is collected with high p_T dilepton triggers; for this sample we require leptons with $p_T > (20, 10) \text{ GeV}$ (leading lepton $p_T > 20 \text{ GeV}$, trailing lepton $p_T > 10 \text{ GeV}$). The second data sample is collected with dilepton- H_T cross triggers; for this sample we require leptons with $p_T > (10, 5) \text{ GeV}$. This is motivated by our desire to maintain sensitivity to possible SUSY signals with relatively low p_T leptons generated in the cascade decays of heavy objects.
 2. The top analysis requires at least two jets of $p_T > 30 \text{ GeV}$ with $E_T^{\text{miss}} > 30 \text{ GeV}$ (ee and $e\mu$) or $E_T^{\text{miss}} > 20 \text{ GeV}$ ($\mu\mu$). We tighten the E_T^{miss} cut to 50 GeV and we also require that the scalar sum of the p_T of all jets with $p_T > 30 \text{ GeV}$ be $> 100 \text{ GeV}$. These requirements considerably reduce backgrounds to the $t\bar{t}$ sample, *e.g.*, backgrounds from Drell Yan and W +jets.
- The pre-selection consists mostly of $t\bar{t}$ events. We perform data – Monte Carlo comparisons of kinematical distributions. Assuming reasonable agreement for the bulk of $t\bar{t}$ we move on to a search for new physics in the tail of the $t\bar{t}$.
- Our prejudice is that new physics would manifest itself in an excess of events with high E_T^{miss} and significant hadronic activity. We define a a-priori search regions by tightening the E_T^{miss} and hadronic activity requirements.
- We perform a counting experiment in the signal regions. We compare observed yields with expectations from Monte Carlo and with three independent data driven techniques (see Sections 9.1, 9.2 and 9.3).

2 Datasets, Triggers, Luminosity

We use the following datasets, and official golden json file (204 pb^{-1}):

Cert_160404-163869.7TeV_May10ReReco_Collisions11.JSON.txt

We use two data samples, one collected with high p_T dilepton triggers and the other with dilepton- H_T cross triggers. These samples are complementary, since the dilepton- H_T trigger sample extends to lower lepton p_T , while the high p_T dilepton trigger sample does not include requirements on the hadronic activity in the event. We use the high p_T dilepton trigger sample as the primary sample for this analysis, while the dilepton- H_T trigger sample is used as a crosscheck, and to search for a possible excess of events at low lepton p_T .

Currently we use data reconstructed in CMSSW 4.2.X and Spring11 MC reconstructed in CMSSW 3.11.X. We will update the MC when the Summer11 madgraph MC samples become available.

• Datasets

– High p_T dilepton trigger sample

- * DoubleElectron_Run2011A-May10ReReco-v1_AOD
- * DoubleMu_Run2011A-May10ReReco-v1_AOD
- * MuEG_Run2011A-May10ReReco-v1_AOD

– Dilepton- H_T cross trigger sample

- * ElectronHad_Run2011A-May10ReReco-v1_AOD
- * MuHad_Run2011A-May10ReReco-v1_AOD

- Monte Carlo samples

- TTJets_TuneZ2_7TeV-madgraph-tauola_Spring11-PU_S1_START311_V1G1-v1
- DYToEE_M-10To20_TuneZ2_7TeV-pythia6_Spring11-PU_S1_START311_V1G1-v1
- DYToMuMu_M-10To20_TuneZ2_7TeV-pythia6_Spring11-PU_S1_START311_V1G1-v1
- DYToTauTau_M-10To20_CT10_TuneZ2_7TeV-powheg-pythia-tauola_Spring11-PU_S1_START311_V1G1-v2
- DYToEE_M-20_CT10_TuneZ2_7TeV-powheg-pythia_Spring11-PU_S1_START311_V1G1-v1
- DYToMuMu_M-20_CT10_TuneZ2_7TeV-powheg-pythia_Spring11-PU_S1_START311_V1G1-v1
- DYToTauTau_M-20_CT10_TuneZ2_7TeV-powheg-pythia-tauola_Spring11-PU_S1_START311_V1G1-v1
- DYJetsToLL_TuneD6T_M-50_7TeV-madgraph-tauola_Spring11-PU_S1_START311_V1G1-v1
- WWTo2L2Nu_TuneZ2_7TeV-pythia6_Spring11-PU_S1_START311_V1G1-v1
- WZtoAnything_TuneZ2_7TeV-pythia6-tauola_Spring11-PU_S1_START311_V1G1-v1
- ZZtoAnything_TuneZ2_7TeV-pythia6-tauola_Spring11-PU_S1_START311_V1G1-v1
- WJetsToLNu_TuneZ2_7TeV-madgraph-tauola_Spring11-PU_S1_START311_V1G1-v1
- TToBLNu_TuneZ2_s-channel_7TeV-madgraph_Spring11-PU_S1_START311_V1G1-v1
- TToBLNu_TuneZ2_t-channel_7TeV-madgraph_Spring11-PU_S1_START311_V1G1-v1
- TToBLNu_TuneZ2_tW-channel_7TeV-madgraph_Spring11-PU_S1_START311_V1G1-v1

3 Event Preselection

The purpose of the preselection is to reject backgrounds other than $t\bar{t} \rightarrow$ dileptons. We compare the kinematical properties of this sample with expectations from $t\bar{t}$ Monte Carlo.

The preselection is based on the $t\bar{t}$ analysis [4]. We select events with two opposite sign, well-identified and isolated leptons (ee , $e\mu$, or $\mu\mu$); one of the leptons must have $P_T > 20$ GeV, the other one must have $P_T > 10$ GeV. Events with dilepton mass consistent with $Z \rightarrow ee/\mu\mu$ are rejected. In case of events with more than two such leptons, we select the pair that maximizes the scalar sum of lepton P_T 's. There must be at least two pfjets of $P_T > 30$ GeV and $|\eta| < 3.0$; jets must pass loose `pfJetId` and be separated by $\Delta R > 0.4$ from any lepton with $P_T > 10$ GeV passing the selection. The scalar sum H_T of the P_T of all such jets must exceed 100 GeV, for the dilepton- H_T sample this requirement is increased to 200 GeV since these triggers have large inefficiency below this threshold. Finally $E_T^{\text{miss}} > 50$ GeV (we use `pfmet`). More details are given in the subsections below.

3.1 Event Cleanup

- Require at least one good deterministic annealing (DA) vertex
 - not fake
 - $\text{ndof} > 4$
 - $|\rho| < 2$ cm
 - $|z| < 24$ cm.

3.2 Muon Selection

Muon candidates are RECO muon objects passing the following requirements:

- $p_T > 5$ GeV and $|\eta| < 2.4$
- Global Muon and Tracker Muon
- χ^2/ndof of global fit < 10
- At least 11 hits in the tracker fit
- Impact parameter with respect to the first DA vertex $d_0 < 200 \mu\text{m}$ and $d_z < 1$ cm
- $I_{\text{so}} \equiv E_T^{\text{iso}}/p_T < 0.15$, E_T^{iso} is defined as the sum of transverse energy/momentum deposits in ecal, hcal, and tracker, in a cone of 0.3

- At least one of the hits from the standalone muon must be used in the global fit
- Require tracker $\Delta p_T/p_T < 0.1$. This cut was not in the original top analysis. It is motivated by the observation of poorly measured muons in data with large relative p_T uncertainty, giving significant contributions to the E_T^{miss}

3.3 Electron Selection

Electron candidates are RECO GSF electrons passing the following requirements:

- $p_T > 10$ GeV and $|\eta| < 2.5$.
- Veto electrons with a supercluster in the transition region $1.4442 < |\eta| < 1.556$.
- VBTf90 identification[5] with requirements tightened to match the CaloIdT and TrkIdVL HLT requirements:
 - $\sigma_{i\eta i\eta} < 0.01$ (EB), 0.03 (EE)
 - $\Delta\phi < 0.15$ (EB), 0.10 (EE)
 - $\Delta\eta < 0.007$ (EB), 0.009 (EE)
 - $H/E < 0.1$ (EB), 0.075 (EE)
- Impact parameter with respect to the first DA vertex $d_0 < 400 \mu\text{m}$ and $d_z < 1$ cm.
- $I_{\text{so}} \equiv E_T^{\text{iso}}/p_T < 0.15$. E_T^{iso} is defined as the sum of transverse energy/momentum deposits in ecal, hcal, and tracker, in a cone of 0.3. A 1 GeV pedestal is subtracted from the ecal energy deposition in the EB, however the ecal energy is never allowed to go negative.
- Electrons with a tracker or global muon within ΔR of 0.1 are vetoed.
- The number of missing expected inner hits must be less than two [6].
- Conversion removal via partner track finding: any electron where an additional GeneralTrack is found with $\text{Dist} < 0.02$ cm and $\Delta \cot \theta < 0.02$ is vetoed [6].

The requirements defining the fakeable objects used to estimate the contributions from fake leptons are listed in App. A.

3.4 Invariant mass requirement

We remove e^+e^- and $\mu^+\mu^-$ events with invariant mass between 76 and 106 GeV. We also remove events with invariant mass < 12 GeV, since this kinematical region is not well reproduced in CMS Monte Carlo and to remove Upsilon's.

In addition, we remove $Z \rightarrow \mu\mu\gamma$ candidates with the γ collinear with one of the muons. This is done as follows: if the ecal energy associated with one of the muons is greater than 6 GeV, we add this energy to the momentum of the initial muon, and we recompute the $\mu\mu$ mass. If this mass is between 76 and 106 GeV, the event is rejected.

3.5 Trigger Selection

We do not make any requirements on HLT bits in the Monte Carlo. Instead, as discussed in Section 4, a trigger efficiency weight is applied to each event, based on the trigger efficiencies measured on data (see Sec. 4).

We select data events using the following triggers. An event in the ee channel is required to pass a DoubleElectron trigger, an event in the $\mu\mu$ channel is required to pass a DoubleMu trigger, and an event in the $e\mu$ channel is required to pass a Ele-Mu trigger.

- High p_T dilepton trigger sample
 - HLT_Ele17_CaloIdL_CaloIsoVL_Ele8_CaloIdL_CaloIsoVL

- HLT_DoubleMu7
- HLT_Mu13_Mu7
- HLT_Mu17_Ele8_CaloIdL
- HLT_Mu8_Ele17_CaloIdL
- Lepton H_T cross trigger sample
 - HLT_DoubleMu3_HT150
 - HLT_DoubleMu3_HT160
 - HLT_Mu3_Ele8_CaloIdL_TrkIdVL_HT150
 - HLT_Mu3_Ele8_CaloIdT_TrkIdVL_HT150
 - HLT_Mu3_Ele8_CaloIdL_TrkIdVL_HT160
 - HLT_Mu3_Ele8_CaloIdT_TrkIdVL_HT160
 - HLT_DoubleEle8_CaloIdL_TrkIdVL_HT150
 - HLT_DoubleEle8_CaloIdT_TrkIdVL_HT150
 - HLT_DoubleEle8_CaloIdL_TrkIdVL_HT160
 - HLT_DoubleEle8_CaloIdT_TrkIdVL_HT160

4 Trigger efficiency

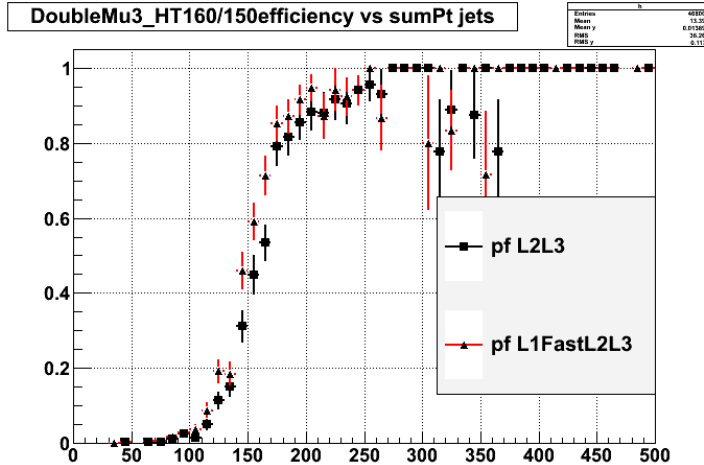


Figure 1: Efficiency for the dimuon- H_T trigger as a function of the offline H_T . The efficiencies with respect to H_T constructed from pfjets with L2L3 vs. L1FastL2L3 corrections are shown (we use the latter). **WILL UPDATE WITH PRETTIER PICTURE COMPARING ee , $\mu\mu$, $e\mu$ TRIGGER EFFICIENCIES.**

For the high p_T dilepton triggers, the efficiencies have been measured to be approximately 100% (DoubleEle), 90% (DoubleMu), and 95% (Mu-Ele) [7]. In the following, unless otherwise specified we weight the ee , $\mu\mu$ and $e\mu$ MC events by these efficiencies. We do not apply any efficiency correction for the hadronic part of the dilepton- H_T triggers. We have verified that the efficiencies for these triggers with respect to an offline selection of $H_T > 200$ GeV is high (~ 90 – 95%), as shown in Fig. 1.

5 Dilepton Yields

The data and MC dilepton mass distributions for events with 2 selected leptons are displayed in Fig. 2. The yields of Z events in the mass range 76–106 GeV are indicated in the figure. In data we observe a 3% excess in the ee channel and a 9% excess in the $\mu\mu$ channel, which we attribute to uncertainties in trigger efficiency, lepton selection efficiency, and integrated luminosity. We use the ratio of $Z \rightarrow \mu^+\mu^-$ to $Z \rightarrow e^+e^-$ yields in data to estimate the ratio of muon to electron selection efficiencies, and find $R_{\mu e} = \text{eff}(\mu)/\text{eff}(e) = 1.12$.

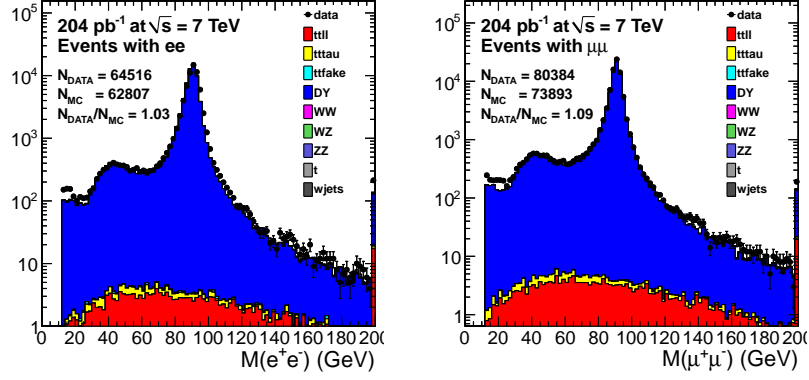


Figure 2: Distributions of dilepton mass in data and MC, in the ee channel (left) and $\mu\mu$ channel (right). The quoted yields refer to events inside the Z mass window 76–106 GeV.

6 Preselection yields

The data yields and the MC predictions for the dilepton trigger sample are given in Table 1. We also look for an excess of low lepton p_T events using the dilepton- H_T trigger sample, and requiring the leptons to pass lepton $p_T > (10, 5)$ GeV but not pass lepton $p_T > (20, 10)$ GeV (to remove overlap with the dilepton trigger sample). Finally, we verify in Table 3 that the data samples collected with high p_T dilepton triggers and lepton- H_T cross triggers give consistent yields, after including the requirements $H_T > 200$ GeV and lepton $p_T > (20, 10)$ GeV.

The MC yields are normalized to 204 pb^{-1} using the cross-sections from Reference [8]. The MC is scaled by the approximate trigger efficiency (100% for ee , 95% for $\mu\mu$, and 95% for $e\mu$) and has been reweighted such that the distribution of reconstructed DA vertices matches that in data. Contributions for $t\bar{t} \rightarrow \text{fake}$ and $W + \text{jets}$ with 1 lepton not originating from W/Z decay (fake lepton) and the contributions from QCD multijet events with 2 fake leptons (single fakes and double fakes, respectively) are estimated with the data-driven fake rate method [4]. **NEED TO APPLY SPILLAGE CORRECTION HERE. IN GENERAL I FIND DATA-DRIVEN FAKES 4 TIMES HIGHER THAN MC, WONDERING IF BUG=TRUE?** The DY contribution is dominated by $DY \rightarrow \tau^+\tau^-$, and we have verified with the data-driven $R_{out/in}$ method [4] that the contributions from $DY \rightarrow e^+e^-$ and $DY \rightarrow \mu^+\mu^-$ are negligible. Also shown are the yields for LM1 and LM3, two of the LM points which are benchmarks for SUSY analyses at CMS. The LM yields are calculated at NLO using process-dependent k-factors computed from Prospino.

As anticipated, the MC predicts that the preselection is dominated by $t\bar{t}$. We observe a slight excess in data with respect to MC expectations.

Table 1: High p_T dilepton trigger data and Monte Carlo yields for the preselection ($n_{\text{jets}} \geq 2$, $H_T > 100$ GeV, $E_T^{\text{miss}} > 50$ GeV, lepton $p_T > (20, 10)$ GeV). For $t\bar{t} \rightarrow \ell^+\ell^-$ and $t\bar{t} \rightarrow \ell^\pm\tau^\mp/\tau^+\tau^-$ $\ell = e, \mu$. **NEED TO APPLY SPILLAGE CORRECTION. SUBTRACT 2 X DOUBLE FAKES FROM SINGLE FAKES. PUT 50% SYST**

Sample	ee	$\mu\mu$	$e\mu$	tot
$t\bar{t} \rightarrow \ell^+\ell^-$	70.3 ± 1.7	77.8 ± 1.7	187.3 ± 2.7	335.4 ± 3.6
$t\bar{t} \rightarrow \ell^\pm\tau^\mp/\tau^+\tau^-$	16.1 ± 0.8	19.5 ± 0.9	42.0 ± 1.3	77.7 ± 1.8
single fakes	8.5 ± 2.2	17.0 ± 3.1	22.7 ± 3.7	48.3 ± 5.3
double fakes	0.0 ± 0.0	0.4 ± 0.3	1.0 ± 0.6	1.5 ± 0.6
DY	3.8 ± 1.0	5.7 ± 1.3	7.9 ± 1.5	17.4 ± 2.2
W^+W^-	0.8 ± 0.1	0.9 ± 0.1	2.0 ± 0.1	3.7 ± 0.2
$W^\pm Z^0$	0.2 ± 0.0	0.2 ± 0.0	0.4 ± 0.0	0.8 ± 0.0
$Z^0 Z^0$	0.1 ± 0.0	0.1 ± 0.0	0.1 ± 0.0	0.2 ± 0.0
single top	2.6 ± 0.1	2.9 ± 0.1	6.9 ± 0.2	12.5 ± 0.3
tot SM MC	102.5 ± 3.1	124.5 ± 3.9	270.4 ± 5.0	497.3 ± 7.1
data	113	122	313	548
LM1	13.1 ± 0.3	14.6 ± 0.3	7.5 ± 0.3	35.1 ± 0.6
LM3	3.0 ± 0.1	3.7 ± 0.1	5.3 ± 0.1	12.0 ± 0.2

Table 2: Dilepton- H_T trigger data and Monte Carlo yields for the preselection (njets ≥ 2 , $H_T > 200$ GeV, $E_T^{\text{miss}} > 50$ GeV, lepton $p_T > (10,5)$ GeV and not lepton $p_T > (20,10)$ GeV). For $t\bar{t} \rightarrow \ell^+\ell^-$ and $t\bar{t} \rightarrow \ell^\pm\tau^\mp/\tau^+\tau^-$ $\ell = e, \mu$. **NEED TO APPLY SPILLAGE CORRECTION. SUBTRACT 2 X DOUBLE FAKES FROM SINGLE FAKES. PUT 50% SYST**

Sample	ee	$\mu\mu$	$e\mu$	tot
$t\bar{t} \rightarrow \ell^+\ell^-$	0.3 ± 0.1	2.2 ± 0.3	2.4 ± 0.3	4.9 ± 0.4
$t\bar{t} \rightarrow \ell^\pm\tau^\mp/\tau^+\tau^-$	0.4 ± 0.1	2.3 ± 0.3	2.1 ± 0.3	4.7 ± 0.4
single fakes	0.0 ± 0.0	3.0 ± 1.2	3.0 ± 1.2	6.0 ± 1.6
double fakes	0.0 ± 0.0	0.6 ± 0.4	0.0 ± 0.0	0.6 ± 0.4
DY	0.0 ± 0.0	2.2 ± 0.8	0.4 ± 0.4	2.6 ± 0.9
W^+W^-	0.0 ± 0.0	0.0 ± 0.0	0.0 ± 0.0	0.0 ± 0.0
$W^\pm Z^0$	0.0 ± 0.0	0.0 ± 0.0	0.0 ± 0.0	0.0 ± 0.0
$Z^0 Z^0$	0.0 ± 0.0	0.0 ± 0.0	0.0 ± 0.0	0.0 ± 0.0
single top	0.0 ± 0.0	0.2 ± 0.0	0.2 ± 0.0	0.4 ± 0.1
tot SM MC	0.7 ± 0.2	10.4 ± 1.5	8.1 ± 1.3	19.3 ± 2.0
data	1	7	5	13
LM1	0.3 ± 0.1	2.9 ± 0.2	2.3 ± 0.1	5.5 ± 0.2
LM3	0.0 ± 0.0	0.4 ± 0.0	0.3 ± 0.0	0.7 ± 0.1

Table 3: Comparison of data yields in the high- p_T dilepton and dilepton- H_T trigger samples, passing the selection njets ≥ 2 , $E_T^{\text{miss}} > 50$ GeV, $H_T > 200$ GeV, lepton $p_T > (20,10)$ GeV.

Sample	ee	$\mu\mu$	$e\mu$	tot
high- p_T dilepton trigger	50	49	124	223
dilepton- H_T trigger	50	48	117	215

7 Properties of data passing the preselection

A number of kinematical distributions for events passing the preselection in data are compared with MC in Appendix C. Although we observe a slight overall excess of data, in general we find that the MC does a good job of reproducing the shapes of the kinematical distributions. Therefore we turn our attention to the tails of the $t\bar{t}$ events.

8 Definition of the signal region

We define signal regions to look for possible new physics contributions in the opposite sign isolated dilepton sample. The choice of signal region is driven by three observations:

1. astrophysical evidence for dark matter suggests that we concentrate on the region of high E_T^{miss} ;
2. new physics signals should have high \sqrt{s} ;
3. observable high cross section new physics signals are likely to be produced strongly; thus, we expect significant hadronic activity in conjunction with the two leptons.

Following these observations, we define the following 3 signal regions by adding requirements of large hadronic activity and missing transverse energy to the preselection of Section 3.

- 2010 signal region: $H_T > 300$ GeV and $y > 8.5 \text{ GeV}^{1/2}$.
- high y signal region: $H_T > 300$ GeV and $y > 13 \text{ GeV}^{1/2}$.
- high H_T signal region: $H_T > 600$ GeV and $y > 8.5 \text{ GeV}^{1/2}$.

We cut on the quantity $y \equiv E_T^{\text{miss}}/\sqrt{H_T}$ rather than E_T^{miss} because the variables H_T and y are largely uncorrelated for the dominant $t\bar{t}$ background. This allows us to use a data-driven ABCD method to estimate the background (see Section 9.1). In the future, we plan to cut instead on E_T^{miss} and H_T , since we observe that E_T^{miss} is a better

discriminant between $t\bar{t}$ vs. SUSY. We have developed a novel technique, which is a variation of the ABCD method, to estimate the background in a signal region defined by E_T^{miss} and H_T requirements (see App. B).

The 2010 signal region is the same as the one used in the 2010 analysis, and was chosen to preserve about 1% of the $t\bar{t}$ sample. The additional signal regions (high y and high H_T) have tightened requirements on y and H_T , respectively, which reduce the expected background by roughly an order of magnitude.

We present the data and MC expected yields in the 3 signal regions in Tables 4-6. Here we require lepton $p_T > (20,10)$ GeV and find the same yields (as well as the same individual events) in the high p_T dilepton trigger and lepton- H_T trigger samples.

Table 4: Data and MC yields in the 2010 signal region. The MC errors are statistical only.

Sample	ee	$\mu\mu$	$e\mu$	tot
$t\bar{t} \rightarrow \ell^+\ell^-$	0.9 ± 0.2	1.4 ± 0.2	2.6 ± 0.3	5.0 ± 0.4
$t\bar{t} \rightarrow \ell^\pm\tau^\mp/\tau^+\tau^-$	0.4 ± 0.1	0.4 ± 0.1	1.2 ± 0.2	2.0 ± 0.3
$t\bar{t} \rightarrow \text{fake}$	0.1 ± 0.1	0.0 ± 0.0	0.2 ± 0.1	0.3 ± 0.1
DY	0.2 ± 0.2	0.4 ± 0.4	0.4 ± 0.4	1.0 ± 0.6
W^+W^-	0.0 ± 0.0	0.0 ± 0.0	0.1 ± 0.0	0.2 ± 0.0
$W^\pm Z^0$	0.0 ± 0.0	0.0 ± 0.0	0.0 ± 0.0	0.0 ± 0.0
$Z^0 Z^0$	0.0 ± 0.0	0.0 ± 0.0	0.0 ± 0.0	0.0 ± 0.0
single top	0.0 ± 0.0	0.0 ± 0.0	0.0 ± 0.0	0.1 ± 0.0
$W + \text{jets}$	0.0 ± 0.0	0.0 ± 0.0	0.0 ± 0.0	0.0 ± 0.0
tot SM MC	1.8 ± 0.3	2.3 ± 0.5	4.5 ± 0.6	8.6 ± 0.8
data	4	3	7	14
LM1	6.4 ± 0.2	7.6 ± 0.2	3.9 ± 0.2	18.0 ± 0.4
LM3	1.3 ± 0.1	1.5 ± 0.1	2.0 ± 0.1	4.8 ± 0.1

Table 5: Data and MC yields in the high y signal region. The MC errors are statistical only.

Sample	ee	$\mu\mu$	$e\mu$	tot
$t\bar{t} \rightarrow \ell^+\ell^-$	0.2 ± 0.1	0.3 ± 0.1	0.5 ± 0.1	0.9 ± 0.2
$t\bar{t} \rightarrow \ell^\pm\tau^\mp/\tau^+\tau^-$	0.0 ± 0.0	0.0 ± 0.0	0.1 ± 0.1	0.2 ± 0.1
$t\bar{t} \rightarrow \text{fake}$	0.0 ± 0.0	0.0 ± 0.0	0.0 ± 0.0	0.0 ± 0.0
DY	0.0 ± 0.0	0.0 ± 0.0	0.0 ± 0.0	0.0 ± 0.0
W^+W^-	0.0 ± 0.0	0.0 ± 0.0	0.0 ± 0.0	0.1 ± 0.0
$W^\pm Z^0$	0.0 ± 0.0	0.0 ± 0.0	0.0 ± 0.0	0.0 ± 0.0
$Z^0 Z^0$	0.0 ± 0.0	0.0 ± 0.0	0.0 ± 0.0	0.0 ± 0.0
single top	0.0 ± 0.0	0.0 ± 0.0	0.0 ± 0.0	0.0 ± 0.0
$W + \text{jets}$	0.0 ± 0.0	0.0 ± 0.0	0.0 ± 0.0	0.0 ± 0.0
tot SM MC	0.2 ± 0.1	0.4 ± 0.1	0.7 ± 0.2	1.3 ± 0.2
data	3	0	3	6
LM1	2.7 ± 0.2	3.2 ± 0.2	1.7 ± 0.1	7.6 ± 0.3
LM3	0.4 ± 0.0	0.5 ± 0.0	0.7 ± 0.1	1.7 ± 0.1

Table 6: Data and MC yields in the high H_T signal region. The errors are statistical only.

Sample	ee	$\mu\mu$	$e\mu$	tot
$t\bar{t} \rightarrow \ell^+ \ell^-$	0.1 ± 0.1	0.2 ± 0.1	0.2 ± 0.1	0.5 ± 0.1
$t\bar{t} \rightarrow \ell^\pm \tau^\mp / \tau^+ \tau^-$	0.1 ± 0.1	0.1 ± 0.1	0.1 ± 0.1	0.2 ± 0.1
$t\bar{t} \rightarrow \text{fake}$	0.0 ± 0.0	0.0 ± 0.0	0.0 ± 0.0	0.0 ± 0.0
DY	0.0 ± 0.0	0.0 ± 0.0	0.4 ± 0.4	0.4 ± 0.4
$W^+ W^-$	0.0 ± 0.0	0.0 ± 0.0	0.0 ± 0.0	0.0 ± 0.0
$W^\pm Z^0$	0.0 ± 0.0	0.0 ± 0.0	0.0 ± 0.0	0.0 ± 0.0
$Z^0 Z^0$	0.0 ± 0.0	0.0 ± 0.0	0.0 ± 0.0	0.0 ± 0.0
single top	0.0 ± 0.0	0.0 ± 0.0	0.0 ± 0.0	0.0 ± 0.0
$W + \text{jets}$	0.0 ± 0.0	0.0 ± 0.0	0.0 ± 0.0	0.0 ± 0.0
tot SM MC	0.2 ± 0.1	0.3 ± 0.1	0.7 ± 0.4	1.2 ± 0.5
data	1	0	2	3
LM1	2.3 ± 0.1	2.7 ± 0.2	1.2 ± 0.1	6.2 ± 0.2
LM3	0.6 ± 0.0	0.6 ± 0.0	0.7 ± 0.1	1.9 ± 0.1

These results are summarized as:

- 2010 signal region ($y > 8.5 \text{ GeV}^{1/2}$, $H_T > 300 \text{ GeV}$)
 - observed yield : 14
 - MC prediction : 8.6 ± 0.8
- high y signal region ($y > 13 \text{ GeV}^{1/2}$, $H_T > 300 \text{ GeV}$)
 - observed yield : 6
 - MC prediction : 1.3 ± 0.2
- high H_T signal region ($y > 8.5 \text{ GeV}^{1/2}$, $H_T > 600 \text{ GeV}$)
 - observed yield : 3
 - MC prediction : 1.2 ± 0.5

For all 3 signal regions, we have verified that we observe the same event yields (and same individual events) in the two data trigger samples. In the 2010 signal region, we observe 14 events, representing a slight excess with respect to the MC expectation. This excess is enhanced after moving to the high y signal region, where we find 6 events. In the high H_T region we observe 3 events, representing a slight excess. A data/MC comparison of the kinematic distributions of the 14 events passing the 2010 signal region selection is presented in App. D.

For all signal regions, we observe 0 events in the Z mass window, confirming the expectation from MC that the DY background is negligible. We also confirm the MC prediction that the contribution of fake leptons is small, using the data-driven fake rate method. We find 1 lepton + fakeable object in the 2010 signal region, giving a predicted contribution from fake leptons of 0.6 ± 0.6 , consistent with MC expectations. For the high y and high H_T signal regions, we do not observe any lepton + fakeable object events and our data-driven prediction for the fake contributions in these regions is zero.

9 Data Driven Background Estimation Methods

For the high p_T dilepton trigger sample, we use 3 data-driven methods to estimate the background in the signal region. The first one exploits the fact that H_T and y are nearly uncorrelated for the $t\bar{t}$ background. The second one is based on the fact that in $t\bar{t}$ the p_T of the dilepton pair is on average nearly the same as the p_T of the pair of neutrinos from W -decays, which is reconstructed as E_T^{miss} in the detector. The third method exploits the fact that in $t\bar{t}$ events the rates of same-flavor vs. opposite-flavor dilepton events are the same. For the low lepton p_T events collected by the dilepton- H_T triggers, we use the opposite-flavor subtraction technique.

We study the closure of these methods using our madgraph $t\bar{t}$ sample, as well as the powheg sample TTTo2L2Nu2B_7TeV-powheg-pythia6.Spring11-PU_S1_START311_V1G1-v1 which has approximately 10 times

more events in the dilepton channel than the madgraph sample. We use these samples to estimate correction factors and systematic uncertainties for the background predictions. However, the final choice of correction factors and uncertainties will be extracted from the Summer11 $t\bar{t}$ madgraph sample which will have 50 times as many events as the current madgraph sample. For the studies presented in this section, we do not apply trigger efficiency corrections or reweighting for number of reconstructed vertices since are not comparing MC to data.

9.1 ABCD method

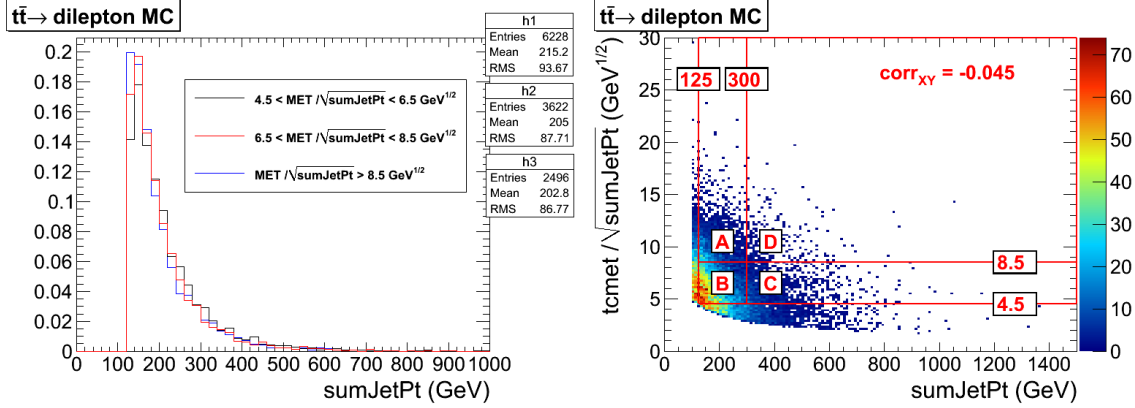


Figure 3: Left: distributions of SumJetPt in MC $t\bar{t}$ events for different intervals of $\text{MET}/\sqrt{\text{SumJetPt}}$. h1, h2, and h3 refer to the $\text{MET}/\sqrt{\text{SumJetPt}}$ intervals 4.5-6.5, 6.5-8.5 and >8.5 , respectively. Right: Distributions of $\text{MET}/\sqrt{\text{SumJetPt}}$ vs. SumJetPt for SM Monte Carlo. Here we also show our choice of ABCD regions. The correlation coefficient corr_{xy} is computed for events falling in the ABCD regions. **THESE PLOTS ARE OLD MC, WILL UPDATE**

We find that in $t\bar{t}$ events H_T and y are nearly uncorrelated, as demonstrated in Fig. 3 (left). Thus, we can use an ABCD method in the y vs. H_T plane to estimate the background in a data driven way. We define 4 regions in the plane of y vs. H_T , as shown in Fig. 3 (right). The region D is the signal region, and the regions A, B and C are control regions. The predicted background in region D is given by $N_A \times N_C / N_B$.

In Table 7, we quote the $t\bar{t}$ MC expected yields for 1 fb^{-1} . In general we find that the prediction agrees with the observed yield in the signal region within $\sim 30\text{-}50\%$ for all signal regions. We also study the dependence of the ratio of observed to predicted signal yields, as a function of the y and H_T requirements used to define the signal region, shown in Fig. 4. Based on these results, we apply the scale factors and uncertainties summarized in Table 9 to the predicted background from the ABCD method.

Table 7: Expected yields from $t\bar{t}$ MC in 1 fb^{-1} in the four ABCD regions for the signal regions depicted in Figs. 6-8, as well as the predicted yield in region D given by $A \times C / B$ and the ratio of the observed signal yield to the prediction. The quoted uncertainties are statistical only.

signal region	sample	A	B	C	D	$A \times B / C$	obs/pred
2010 signal region	madgraph	251.3 ± 6.1	951.5 ± 11.9	165.2 ± 4.9	38.3 ± 2.4	43.6 ± 1.8	0.88 ± 0.07
	powheg	231.7 ± 2.0	850.6 ± 3.7	157.8 ± 1.6	37.0 ± 0.8	43.0 ± 0.6	0.86 ± 0.02
high y signal region	madgraph	18.4 ± 1.6	951.5 ± 11.9	165.2 ± 4.9	4.9 ± 0.9	3.2 ± 0.3	1.53 ± 0.30
	powheg	17.3 ± 0.5	850.6 ± 3.7	157.8 ± 1.6	4.2 ± 0.3	3.2 ± 0.1	1.30 ± 0.09
high H_T signal region	madgraph	251.3 ± 6.1	951.5 ± 11.9	11.1 ± 1.3	3.8 ± 0.8	2.9 ± 0.3	1.31 ± 0.30
	powheg	231.7 ± 2.0	850.6 ± 3.7	12.5 ± 0.5	3.8 ± 0.3	3.4 ± 0.1	1.13 ± 0.08

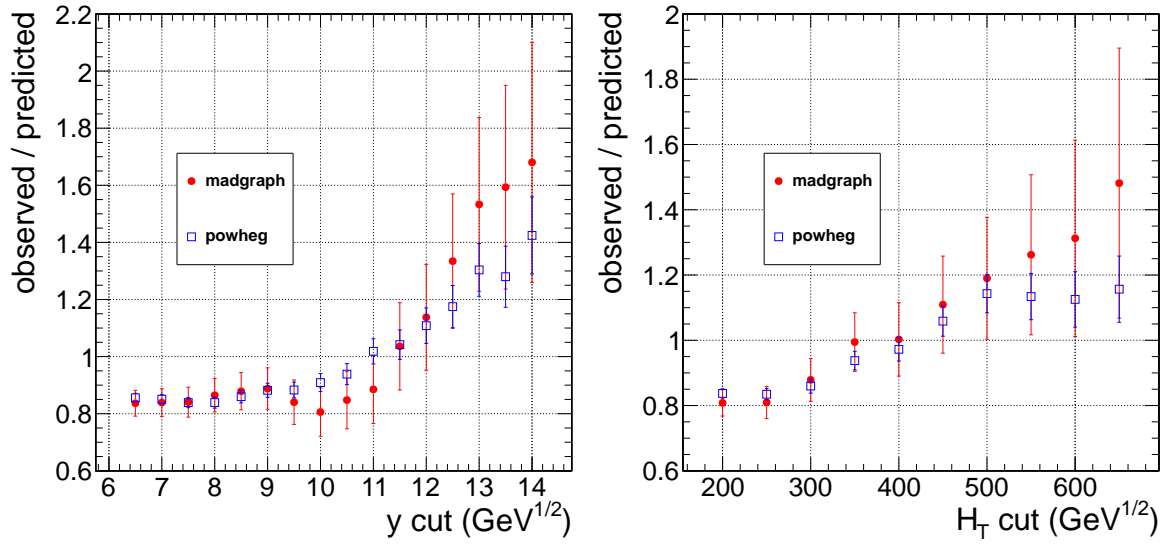


Figure 4: Variation of observed/predicted for the ABCD method as a function of the y and H_T cuts defining the signal region.

9.2 Dilepton P_T method

This method is based on a suggestion by V. Pavlunin[9], and was investigated by our group in 2009[10] and in our 2010 analysis [3]. The idea is that in dilepton $t\bar{t}$ events the lepton and neutrinos from W decays have the same P_T spectrum (modulo W polarization effects). One can then use the observed $P_T(\ell\ell)$ distribution to model the sum of neutrino P_T 's which is identified with the E_T^{miss} .

Then, in order to predict the $t\bar{t} \rightarrow$ dilepton contribution to a selection with $E_T^{\text{miss}} + X$, one applies a cut on $P_T(\ell\ell) + X$ instead. In practice one has to rescale the result of the $P_T(\ell\ell) + X$ selection to account for the fact that any dilepton selection must include a moderate E_T^{miss} cut in order to reduce Drell Yan backgrounds. This is discussed in Section 5.3 of Reference [10]; for a E_T^{miss} cut of 50 GeV, the rescaling factor is obtained from the MC as

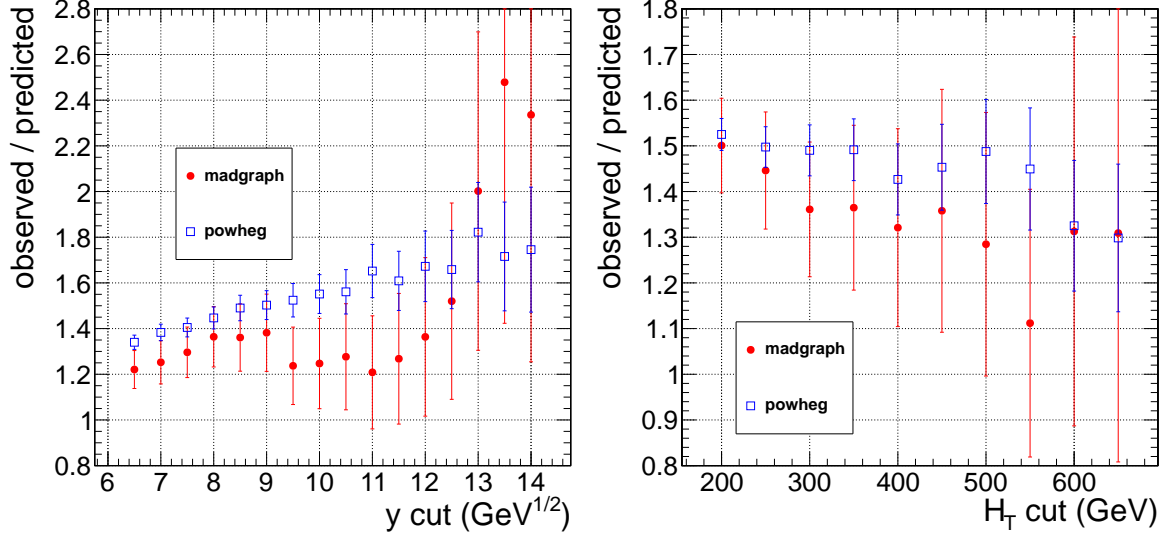


Figure 5: Variation of observed/predicted for the $p_T(\ell\ell)$ method as a function of the y and H_T cuts defining the signal region.

We summarize the expected results of the $p_T(\ell\ell)$ method in 1 fb^{-1} $t\bar{t}$ MC in Table 8, and we show the dependence of observed/predicted vs. the signal region requirements in Fig. 5. Based on these results, we apply the scale factors and uncertainties summarized in Table 9 to the predicted background from the ABCD method. In [2], we have studied extensively the origin of the excess of observed vs. predicted events from this method. We found that it is due mostly to the W polarization, which results in a harder p_T distribution for the W neutrinos than charged leptons.

Table 8: Expected observed and predicted yields in 1 fb^{-1} for $t\bar{t}$ MC for the $p_T(\ell\ell)$ method, and the ratio of the observed signal yield to the prediction. The quoted uncertainties are statistical only, assuming Gaussian errors.

signal region	sample	predicted	observed	obs/pred
2010 signal region	madgraph	28.2 ± 2.5	38.3 ± 2.4	1.36 ± 0.15
	powheg	24.8 ± 0.8	37.0 ± 0.8	1.49 ± 0.06
high y signal region	madgraph	2.4 ± 0.7	4.9 ± 0.9	2.00 ± 0.70
	powheg	2.3 ± 0.2	4.2 ± 0.3	1.82 ± 0.22
high H_T signal region	madgraph	2.9 ± 0.8	3.8 ± 0.8	1.31 ± 0.43
	powheg	2.9 ± 0.2	3.8 ± 0.3	1.33 ± 0.14

$$K = \frac{\int_0^\infty \mathcal{N}(p_T(\ell\ell)) dp_T(\ell\ell)}{\int_{50}^\infty \mathcal{N}(p_T(\ell\ell)) dp_T(\ell\ell)} = 1.5$$

Table 9: Summary of correction factors and systematic uncertainties for the ABCD and $p_T(\ell\ell)$ methods in the 3 signal regions.

signal region	ABCD	$p_T(\ell\ell)$
2010 signal region	1.0 ± 0.2	1.4 ± 0.2
high y signal region	1.3 ± 0.3	1.7 ± 0.3
high H_T signal region	1.2 ± 0.2	1.3 ± 0.2

9.3 Opposite-Flavor Subtraction

The opposite-flavor subtraction technique exploits the fact that in $t\bar{t}$, the flavor of the 2 leptons from W decay are uncorrelated. Hence we expect equal rates of same-flavor (SF) ee or $\mu\mu$ vs. opposite-flavor (OF) $e\mu$ lepton pairs. In SUSY, the lepton flavors may be correlated, producing an excess of SF over OF events. We use the observed yield in the OF final state to predict the yields in the SF final state according to:

$$N(ee) = \frac{1}{2R_{\mu e}}N(e\mu) \text{ and } N(\mu\mu) = \frac{R_{\mu e}}{2}N(e\mu)$$

where $R_{\mu e}$ is the ratio of muon to electron selection efficiencies. This quantity is evaluated by taking the ratio of the number of observed $Z \rightarrow \mu^+\mu^-$ to $Z \rightarrow e^+e^-$ events, in the mass range 76-106 GeV with no jets or E_T^{miss} requirements (see Fig. 2). Alternatively, we can quantify the excess of SF vs. OF events with the quantity:

$$\Delta = R_{\mu e}N(ee) + \frac{1}{R_{\mu e}}N(\mu\mu) - N(e\mu),$$

which is predicted to be 0 for processes with uncorrelated lepton flavors. In order for this technique to work, the kinematic selection applied to events in all dilepton flavor channels must be the same, which is not the case for our default selection because the Z mass veto is applied only to same-flavor channels. Therefore when applying the OF subtraction technique we also apply the Z mass veto also to the $e\mu$ channel.

We will apply this technique to both the high p_T dilepton trigger and dilepton- H_T trigger data samples. In the following, we first apply the technique to $t\bar{t}$ MC with high p_T leptons, and then to $t\bar{t}$ MC with low p_T leptons.

9.3.1 OF subtraction: Application to high p_T lepton sample

We begin by applying the OF subtraction technique to $t\bar{t}$ MC with leptons passing $p_T > (20,10)$ GeV. Here we extract $R_{e\mu}$ by taking the ratio of $Z \rightarrow \mu^+\mu^-$ vs. $Z \rightarrow e^+e^-$ events in the window 76-106 GeV in DY MC. The results are summarized in Table 10, where we find values of Δ consistent with 0, as expected.

Table 10: Expected yields in $1 \text{ fb}^{-1} t\bar{t}$ MC for the OF subtraction method, and the quantity $\Delta = R_{\mu e}N(ee) + \frac{1}{R_{\mu e}}N(\mu\mu) - N(e\mu)$. The quoted systematic uncertainty refers to that of $R_{\mu e}$.

region	sample	$N(ee)$	$N(\mu\mu)$	$N(e\mu)$	Δ
preselection region	madgraph	431.1 ± 8.0	531.3 ± 8.9	945.8 ± 11.8	$11.8 \pm 16.8 \text{ (stat)} \pm 1.1 \text{ (syst)}$
	powheg	383.1 ± 2.5	492.9 ± 2.9	876.2 ± 3.8	$-7.0 \pm 5.4 \text{ (stat)} \pm 0.8 \text{ (syst)}$
2010 signal region	madgraph	7.4 ± 1.0	10.7 ± 1.3	14.5 ± 1.5	$3.3 \pm 2.2 \text{ (stat)} \pm 0.04 \text{ (syst)}$
	powheg	7.2 ± 0.3	8.6 ± 0.4	16.8 ± 0.5	$-1.1 \pm 0.7 \text{ (stat)} \pm 0.03 \text{ (syst)}$

9.3.2 OF subtraction: Application to low p_T lepton sample

ADD CLOSURE STUDIES OF OF SUBTRACTION WITH TT MC LOW PT LEPTONS

10 Results

10.1 Background estimate from the ABCD method

The data yields in the four regions are summarized in Tables 11-Table 13 for the 3 signal regions. The ABCD background prediction $N_A \times N_C/N_B$ is scaled by the correction factors determined in Sec. 9, as summarized in Table 9. The results of the ABCD predictions are summarized in Table 14.

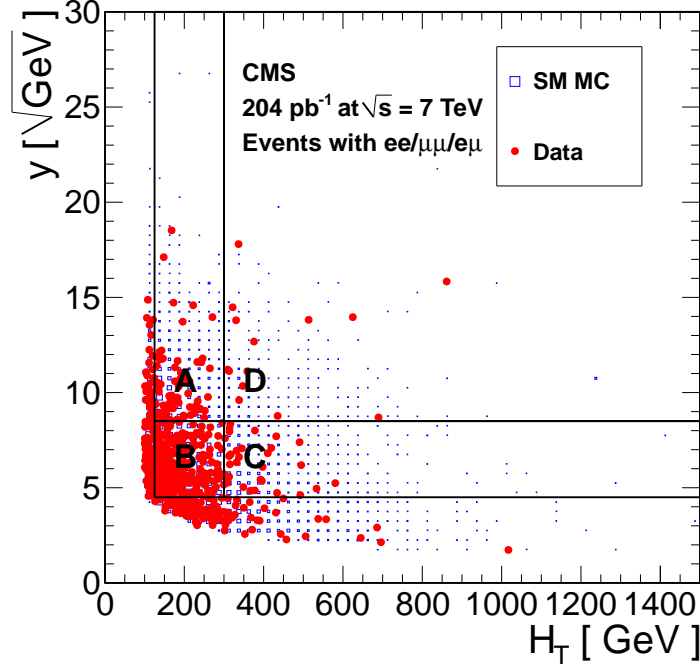


Figure 6: Distributions of y vs. H_T for SM Monte Carlo and data. The 2010 signal region boundaries are overlaid.

Table 11: Data yields in the four regions of Figure 6 for the 2010 signal region, as well as the predicted yield in region D given by $A \times C / B$. The quoted uncertainty on the prediction in data is statistical only, assuming Gaussian errors. We also show the SM Monte Carlo expectations with statistical errors only.

sample	A	B	C	D	$A \times B / C$
$t\bar{t}$	48.8 ± 1.4	184.1 ± 2.7	31.9 ± 1.1	7.3 ± 0.5	8.5 ± 0.4
DY	0.5 ± 0.4	8.2 ± 1.5	0.7 ± 0.5	1.0 ± 0.6	0.0 ± 0.0
W^+W^-	0.6 ± 0.1	1.6 ± 0.1	0.1 ± 0.0	0.2 ± 0.0	0.1 ± 0.0
$W^\pm Z^0$	0.1 ± 0.0	0.3 ± 0.0	0.0 ± 0.0	0.0 ± 0.0	0.0 ± 0.0
$Z^0 Z^0$	0.0 ± 0.0	0.1 ± 0.0	0.0 ± 0.0	0.0 ± 0.0	0.0 ± 0.0
single top	1.9 ± 0.1	5.6 ± 0.2	0.2 ± 0.0	0.1 ± 0.0	0.1 ± 0.0
$W + \text{jets}$	0.6 ± 0.6	1.2 ± 0.6	0.0 ± 0.0	0.0 ± 0.0	0.0 ± 0.0
Total SM MC	52.6 ± 1.6	201.2 ± 3.2	33.1 ± 1.2	8.6 ± 0.8	8.6 ± 0.4
data	72	238	29	14	8.8 ± 2.0

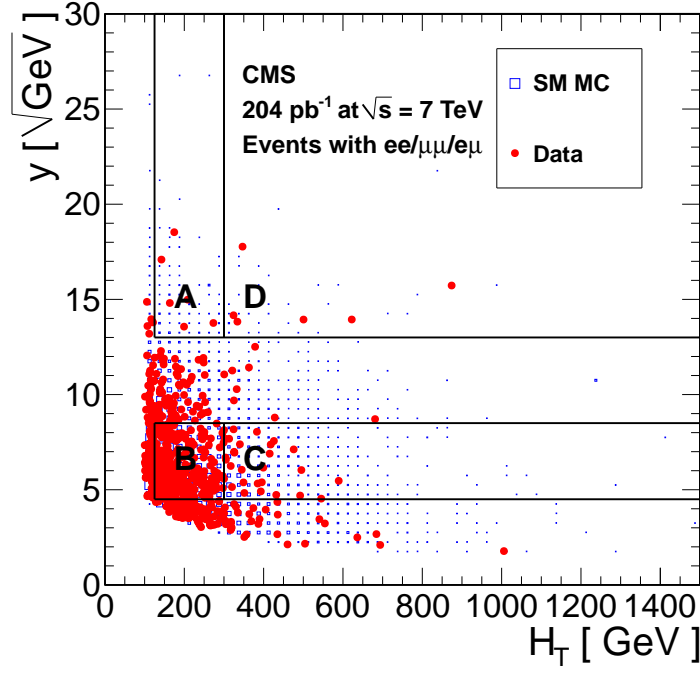


Figure 7: Distributions of y vs. H_T for SM Monte Carlo and data. The high y signal region boundaries are overlaid.

Table 12: Data yields in the four regions of Figure 7 for the high y signal region, as well as the predicted yield in region D given by $A \times C / B$. The quoted uncertainty on the prediction in data is statistical only, assuming Gaussian errors. We also show the SM Monte Carlo expectations with statistical uncertainties.

sample	A	B	C	D	$A \times B / C$
$t\bar{t}$	3.6 ± 0.4	184.1 ± 2.7	31.9 ± 1.1	1.2 ± 0.2	0.6 ± 0.1
DY	0.3 ± 0.3	8.2 ± 1.5	0.7 ± 0.5	0.0 ± 0.0	0.0 ± 0.0
W^+W^-	0.1 ± 0.0	1.6 ± 0.1	0.1 ± 0.0	0.1 ± 0.0	0.0 ± 0.0
$W^\pm Z^0$	0.0 ± 0.0	0.3 ± 0.0	0.0 ± 0.0	0.0 ± 0.0	0.0 ± 0.0
$Z^0 Z^0$	0.0 ± 0.0	0.1 ± 0.0	0.0 ± 0.0	0.0 ± 0.0	0.0 ± 0.0
single top	0.2 ± 0.0	5.6 ± 0.2	0.2 ± 0.0	0.0 ± 0.0	0.0 ± 0.0
$W + \text{jets}$	0.0 ± 0.0	1.2 ± 0.6	0.0 ± 0.0	0.0 ± 0.0	0.0 ± 0.0
Total SM MC	4.1 ± 0.5	201.2 ± 3.2	33.1 ± 1.2	1.3 ± 0.2	0.7 ± 0.1
data	6	238	29	6	0.7 ± 0.3

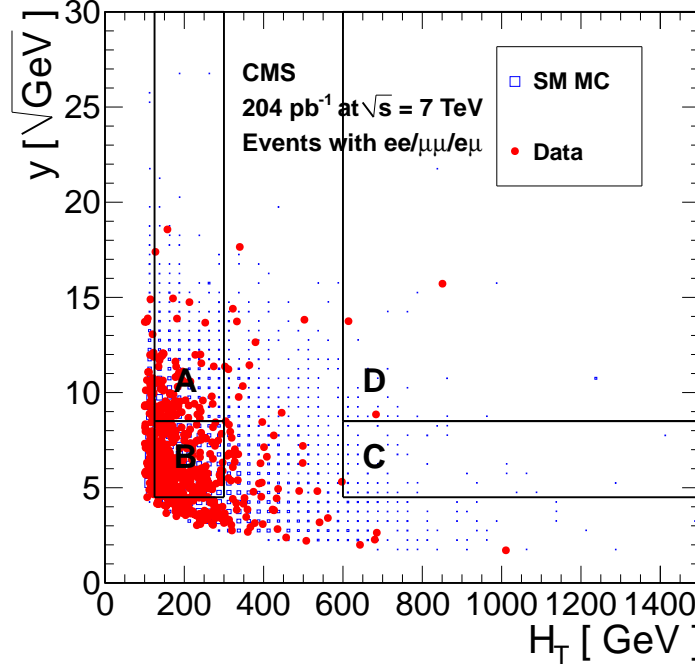


Figure 8: Distributions of y vs. H_T for SM Monte Carlo and data. The high H_T signal region boundaries are overlaid.

Table 13: Data yields in the four regions of Figure 8 for the high H_T signal region, as well as the predicted yield in region D given by $A \times C / B$. The quoted uncertainty on the prediction in data is statistical only, assuming Gaussian errors. Since the yield in region C is 0, we assess as the uncertainty the prediction corresponding to 1 observed event in 1. We also show the SM Monte Carlo expectations with statistical uncertainties.

sample	A	B	C	D	$A \times B / C$
ttall	48.8 ± 1.4	184.1 ± 2.7	2.2 ± 0.3	0.7 ± 0.2	0.6 ± 0.1
DY	0.5 ± 0.4	8.2 ± 1.5	0.0 ± 0.0	0.4 ± 0.4	0.0 ± 0.0
WW	0.6 ± 0.1	1.6 ± 0.1	0.0 ± 0.0	0.0 ± 0.0	0.0 ± 0.0
WZ	0.1 ± 0.0	0.3 ± 0.0	0.0 ± 0.0	0.0 ± 0.0	0.0 ± 0.0
ZZ	0.0 ± 0.0	0.1 ± 0.0	0.0 ± 0.0	0.0 ± 0.0	0.0 ± 0.0
t	1.9 ± 0.1	5.6 ± 0.2	0.0 ± 0.0	0.0 ± 0.0	0.0 ± 0.0
wjets	0.6 ± 0.6	1.2 ± 0.6	0.0 ± 0.0	0.0 ± 0.0	0.0 ± 0.0
Total SM MC	52.6 ± 1.6	201.2 ± 3.2	2.2 ± 0.3	1.2 ± 0.5	0.6 ± 0.1
data	72	238	0	3	0.0 ± 0.3

Table 14: Summary of results of the ABCD method, applied to the 3 signal regions.

Signal Region	$N_A \times N_C/N_B$	correction factor	prediction
2010 signal region	8.8 ± 2.0	1.0 ± 0.2	8.8 ± 2.0 (stat) ± 1.8 (syst)
high y signal region	0.7 ± 0.3	1.3 ± 0.2	0.9 ± 0.4 (stat) ± 0.2 (syst)
high H_T signal region	0.0 ± 0.3	1.2 ± 0.2	0.0 ± 0.4 (stat) ± 0.1 (syst)

10.2 Background estimate from the $P_T(\ell\ell)$ method

Table 15: Summary of results of the dilepton p_T template method. The quantities indicated in the table are discussed in the text. The quoted statistical uncertainty in the prediction N_P is due to that of $N(D')$, the quoted systematic uncertainty includes that of $N(DY)$ and K_C . **K and KC taken from MC, do we want to take K and/or KC from data? Need to add jet/met uncertainty here**

Signal Region	$N(D')$	$N(DY)$	K	K_C	N_P
2010 signal region	3	0.4 ± 0.3	1.5	1.4 ± 0.2	5.5 ± 3.6 (stat) ± 1.0 (syst)
high y signal region	2	0.1 ± 0.1	1.5	1.7 ± 0.3	4.8 ± 3.6 (stat) ± 0.9 (syst)
high H_T signal region	0	0.0 ± 0.1	1.3	1.3 ± 0.2	0.0 ± 1.7 (stat) ± 0.3 (syst)

For each signal region D, we count the number of events falling in the region D', which is defined using the same requirements as D but switching the y requirement to a $p_T(\ell\ell)/\sqrt{H_T}$ requirement. We subtract off the expected DY contribution using the data-driven $R_{out/in}$ technique, using $R_{out/in} = 0.13 \pm 0.07$. **add plot justifying this value.** We then scale this yield by 2 corrections factors: K , the E_T^{miss} acceptance correction factor, and K_C , the correction factor determined in Sec. 9. Our final prediction N_P is given by the following, as summarized in Table 15:

$$N_P = (N(D') - N(DY)) \times K \times K_C.$$

I will add here the results of victory method applied to the H_T sideband region as a validation of the method and victory plots.

10.3 Background estimate from OF subtraction

The results of the OF subtraction technique are summarized in Table 16. We evaluate the quantity $\Delta = R_{\mu e}N(ee) + \frac{1}{R_{\mu e}}N(\mu\mu) - N(e\mu)$ with $R_{\mu e} = 1.12 \pm 0.05$ extracted from the ratio of $Z \rightarrow \mu^+\mu^-$ vs. $Z \rightarrow e^+e^-$ events in data. We perform the OF subtraction first in the preselection region, and find Δ consistent with 0, as expected. We then perform the OF subtraction in all 3 signal regions, and do not observe any excess of same-flavor vs. opposite-flavor events.

Table 16: Summary of results for the OF subtraction technique. The quantity $\Delta = R_{\mu e}N(ee) + \frac{1}{R_{\mu e}}N(\mu\mu) - N(e\mu)$ is quoted with $R_{\mu e} = 1.12 \pm 0.05$. The quoted systematic uncertainty corresponds to that of $R_{\mu e}$. The $e\mu$ yields differ from those previously quoted because the Z mass veto is included here.

region	$N(ee)$	$N(\mu\mu)$	$N(e\mu)$	Δ
preselection region	113	122	258	-22.5 ± 22.3 (stat) ± 0.8 (syst)
2010 signal region	4	3	5	2.2 ± 3.5 (stat) ± 0.1 (syst)
high y signal region	3	0	2	1.4 ± 2.4 (stat) ± 0.1 (syst)
high H_T signal region	1	0	1	0.1 ± 1.5 (stat) ± 0.0 (syst)

10.4 Summary of results

A summary of our results is presented in Table 17. We observe a slight excess of events with respect to MC and data-driven predictions in our loose 2010 signal region. The excess with respect to MC and ABCD predictions is enhanced after tightening the y requirement, but the observed yield shows no significant excess with respect to the $p_T(\ell\ell)$ method prediction. There is also a slight excess of events with respect to MC and data-driven predictions for the high H_T signal region. We do not observe any excess of same-flavor vs. opposite-flavor events.

Table 17: Summary of the observed and predicted yields in the 3 signal regions. MC errors are statistical only. The systematic uncertainty on the ABCD and $p_T(\ell\ell)$ method is from the scaling factors from MC closure only **need to put additional uncertainties, for example jet/met scale**. For the OF subtraction, the quantity $\Delta = R_{\mu e}N(ee) + \frac{1}{R_{\mu e}}N(\mu\mu) - N(e\mu)$ is quoted; the systematic uncertainty here is from the ratio of muon to electron selection efficiencies.

	2010 signal region	high y signal region	high H_T signal region
Observed yield	14	6	3
MC prediction	8.6 ± 0.8	1.3 ± 0.2	1.2 ± 0.5
ABCD prediction	8.8 ± 2.0 (stat) ± 1.8 (syst)	0.9 ± 0.4 (stat) ± 0.2 (syst)	0.0 ± 0.4 (stat) ± 0.1 (syst)
$p_T(\ell\ell)$ prediction	5.5 ± 3.6 (stat) ± 1.0 (syst)	4.8 ± 3.6 (stat) ± 0.9 (syst)	0.0 ± 1.7 (stat) ± 0.3 (syst)
OF subtraction (Δ)	2.2 ± 3.5 (stat) ± 0.1 (syst)	1.4 ± 2.4 (stat) ± 0.1 (syst)	0.1 ± 1.5 (stat) ± 0.0 (syst)

References

- [1] ADD REF TO MET TEMPLATES NOTE, WHEN AVAILABLE
- [2] CMS AN-2010/370
- [3] arXiv:1103.1348v1 [hep-ex], “Search for Physics Beyond the Standard Model in Opposite-Sign Dilepton Events at $\sqrt{s} = 7$ TeV.”
- [4] Phys.Lett.B695:424-443,2011
- [5] <https://twiki.cern.ch/twiki/bin/viewauth/CMS/SimpleCutBasedEleID>
- [6] D. Barge *et al.*, AN-CMS2009/159.
- [7] CMS AN-2011/155
- [8] <https://twiki.cern.ch/twiki/bin/view/CMS/ProductionReProcessingSpring10>
- [9] V. Pavlunin, Phys. Rev. **D81**, 035005 (2010).
- [10] D. Barge *et al.*, AN-CMS2009/130.
- [11] W. Andrews *et al.*, AN-CMS2009/023.
- [12] D. Barge *et al.*, AN-CMS2010/257.
- [13] W. Andrews *et al.*, AN-CMS2010/274.
- [14] J. Conway, <http://www-cdf.fnal.gov/physics/statistics/code/bayes.f>.
- [15] G. Landsberg, <https://twiki.cern.ch/twiki/pub/CMS/EXOTICA/cl95cms.c>
- [16] <https://hypernews.cern.ch/HyperNews/CMS/get/susy/617/2/1.html>
- [17] <https://twiki.cern.ch/twiki/bin/view/CMS/SUSY38XSUSYScan>
- [18] arXiv:hep-ph/0605240v2
- [19] CleanExclusion.cc available at <https://twiki.cern.ch/twiki/bin/viewauth/CMS/SUSYLimitTools>
- [20] R. Cousins, http://www.physics.ucla.edu/~cousins/stats/cousins_lognormal_prior.pdf
- [21] S. Harper, private communication (relayed to us by M. Chiorboli.).
- [22] A. Barr *et al.*, J.Phys.G29:2343-2363,2003; Cheng, H.C., Han, arXiv:hep-ph/0810.5178v2.
<http://indico.cern.ch/contributionDisplay.py?contribId=3&confId=66410>
- [23] <http://indico.cern.ch/contributionDisplay.py?contribId=5&confId=93837>
- [24] M. Narain *et al.*, CMS AN-2010/259; we thank the Brown group for providing their code to us.

Appendix A Fakeable Object Definitions

We estimate the contributions from leptons not originating from W/Z decay (fake leptons) using the data-driven fake rate method [4]. We define the following ‘fakeable object’ selections, by taking the electron and muon requirements listed in Sec. 3 and loosening the following requirements:

- electrons

- $d_0 < 0.2$ cm

- $Iso \equiv E_T^{iso}/p_T < 0.4$, E_T^{iso} is defined as the sum of transverse energy/momentum deposits in ecal, hcal, and tracker, in a cone of 0.3 A 1 GeV pedestal is subtracted from the ecal energy deposition in the EB, however the ecal energy is never allowed to go negative.

- muons

- $d_0 < 0.2$ cm

- χ^2/ndof of global fit < 50

- $Iso \equiv E_T^{iso}/p_T < 0.4$, E_T^{iso} is defined as the sum of transverse energy/momentum deposits in ecal, hcal, and tracker, in a cone of 0.3

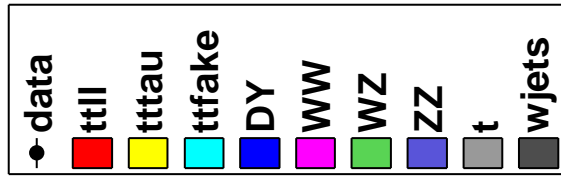
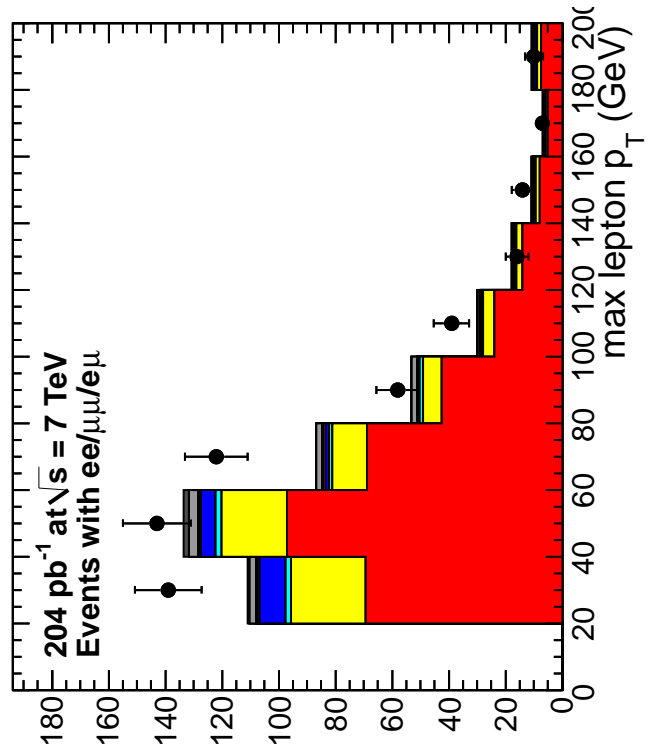
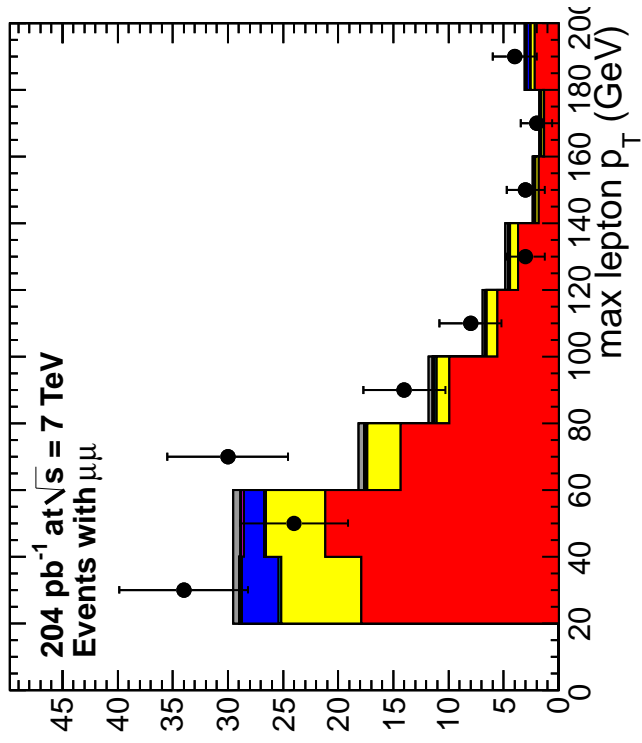
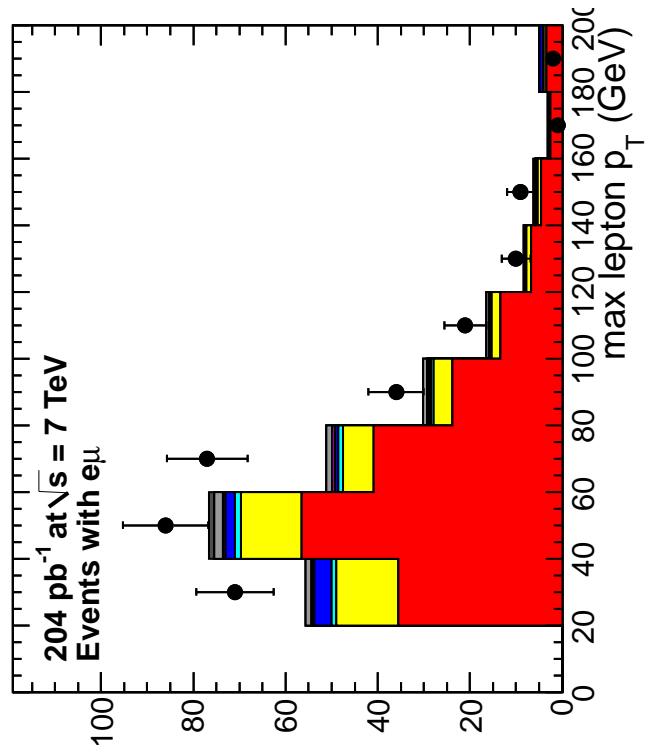
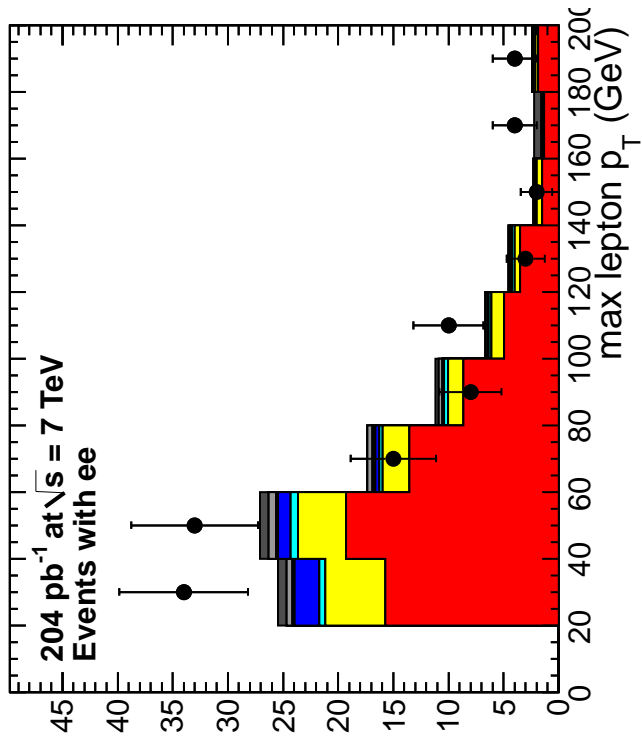
Appendix B The ABCD’ Method

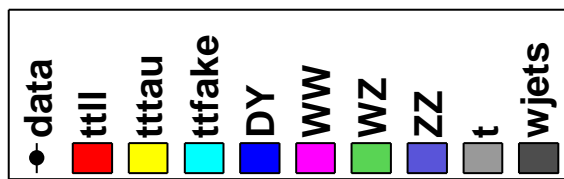
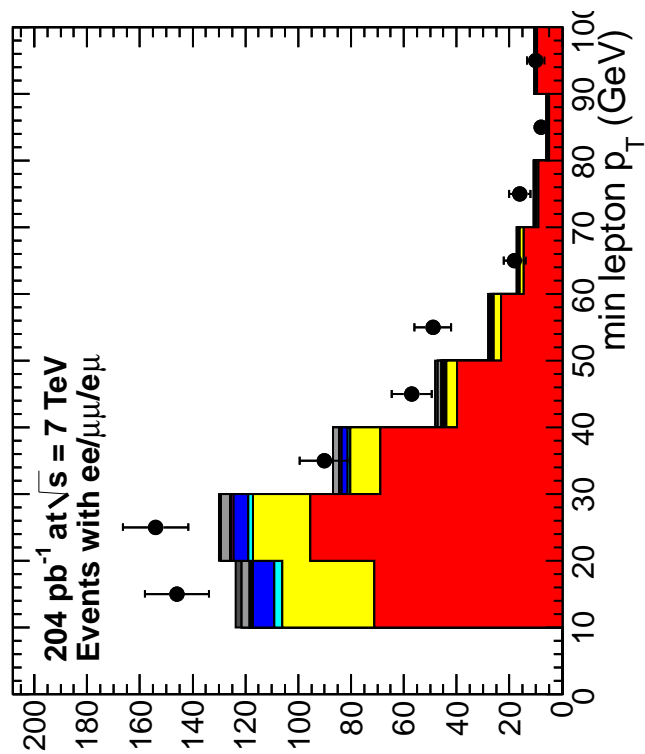
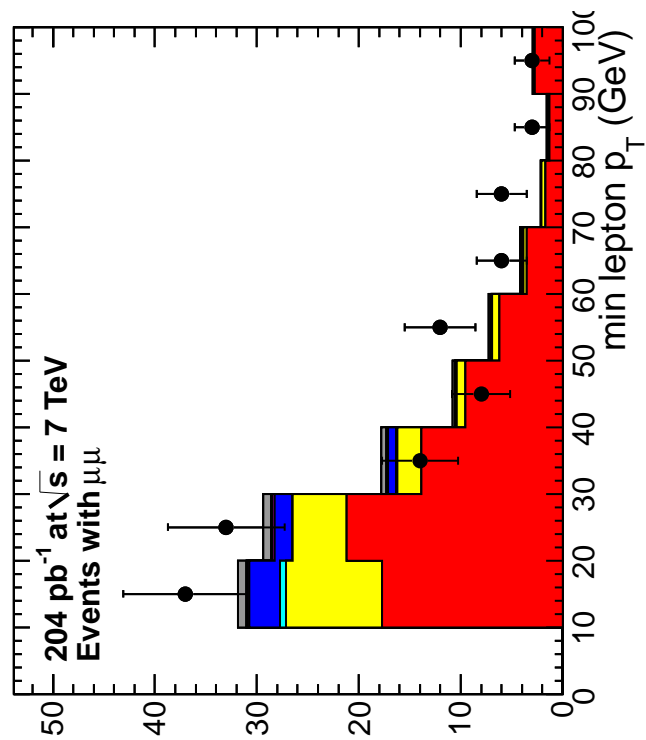
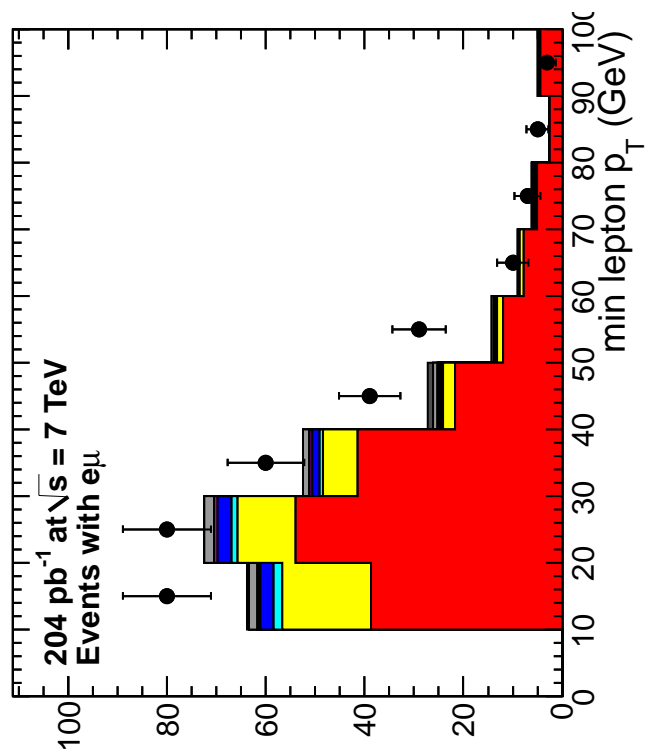
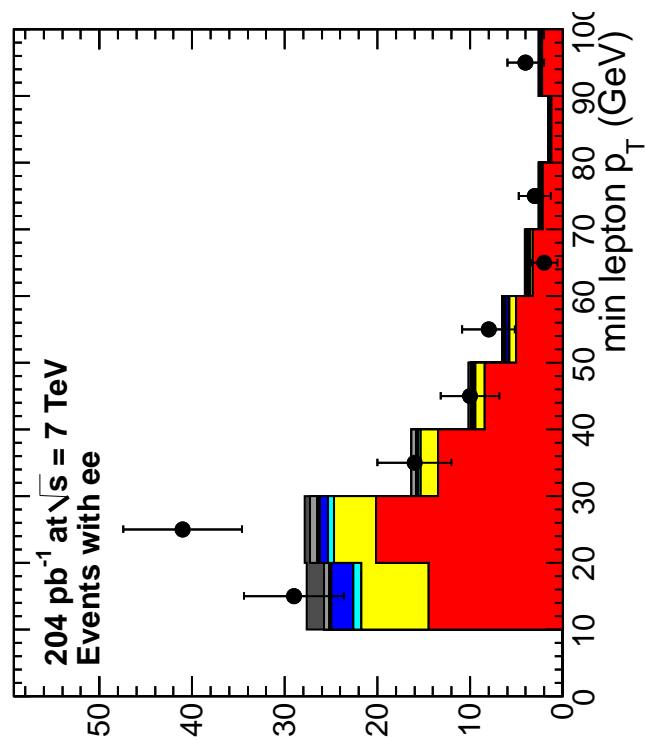
Appendix C Data/MC Comparison: Preselection Region

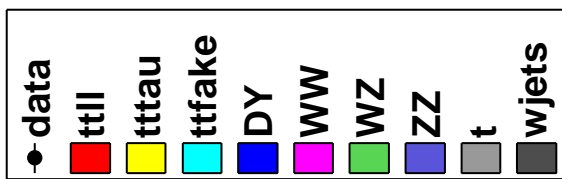
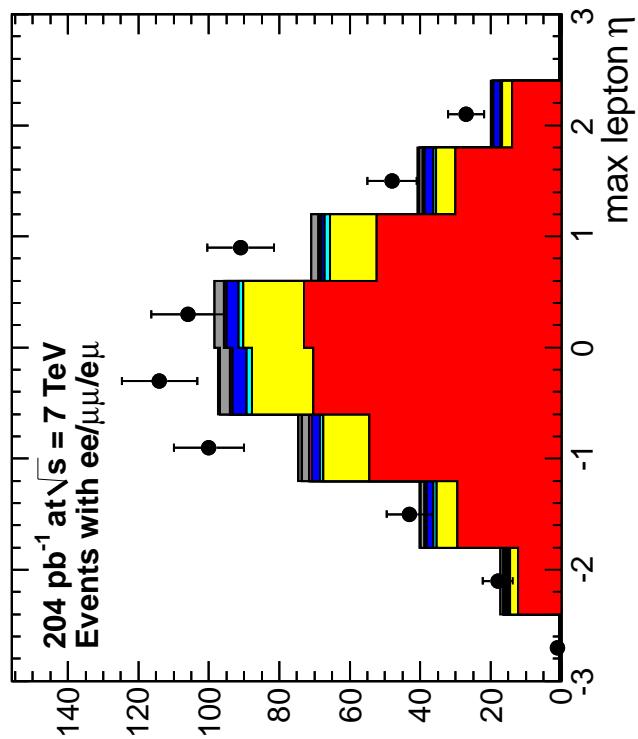
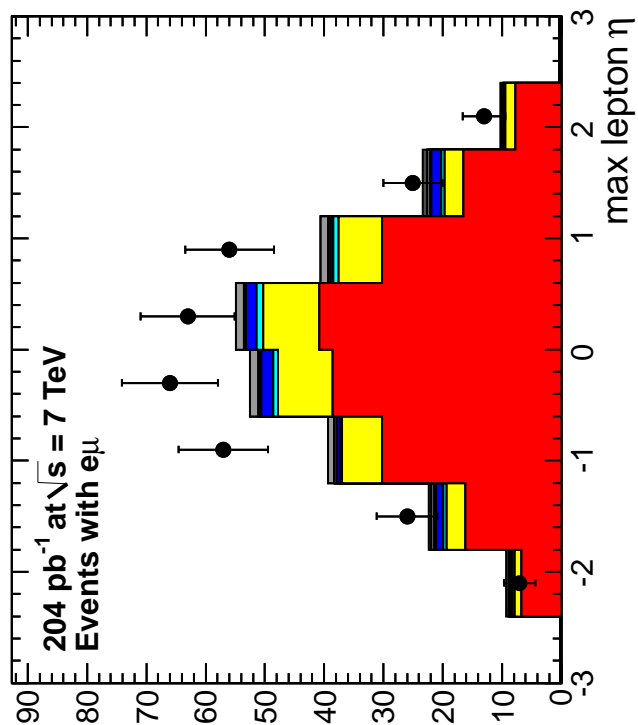
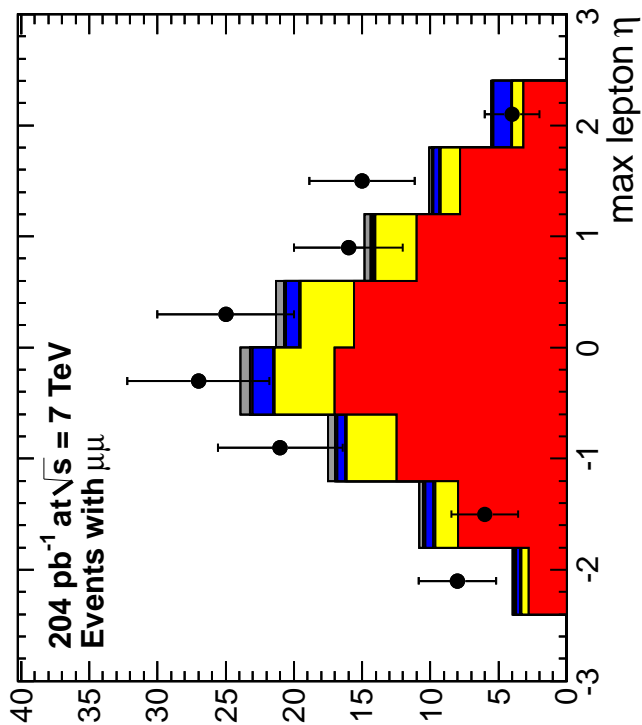
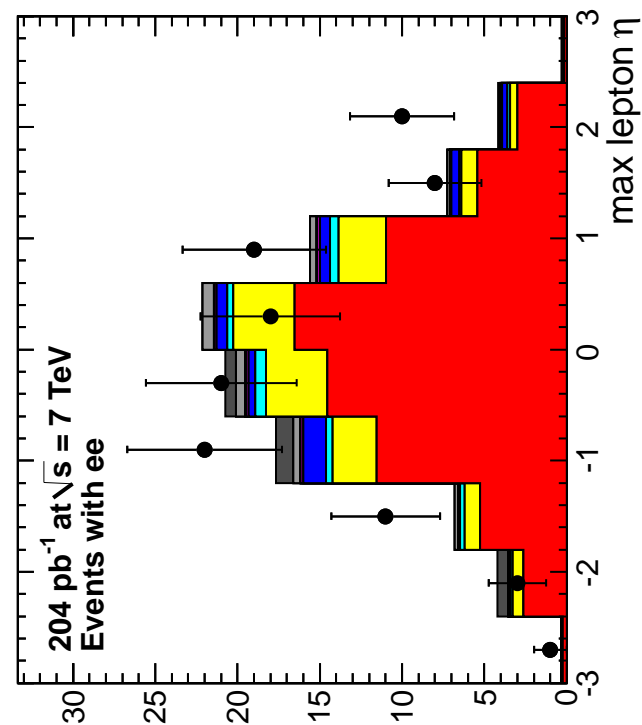
Here we compare data and MC distributions for data passing the preselection requirements. The high p_T dilepton trigger data is used.

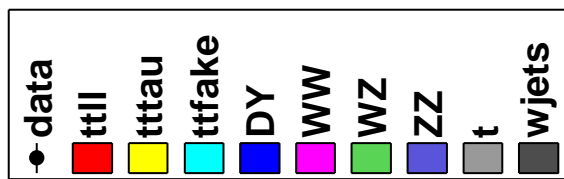
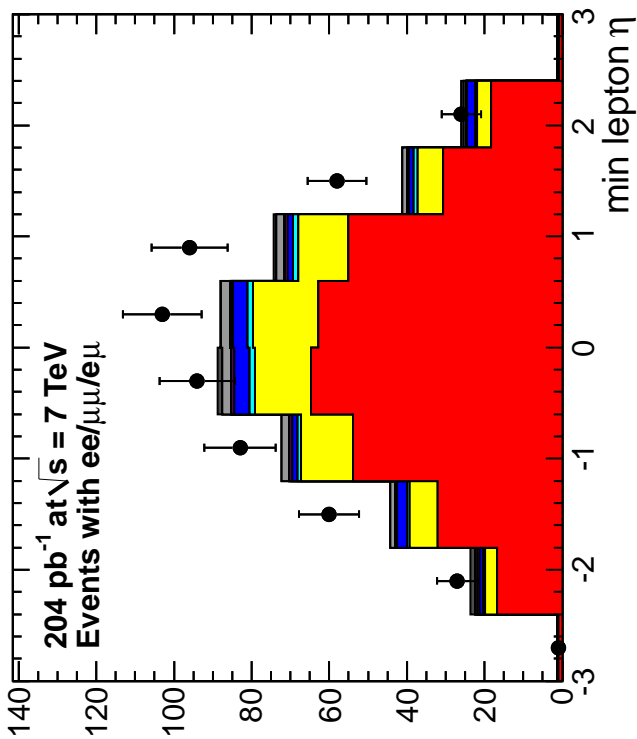
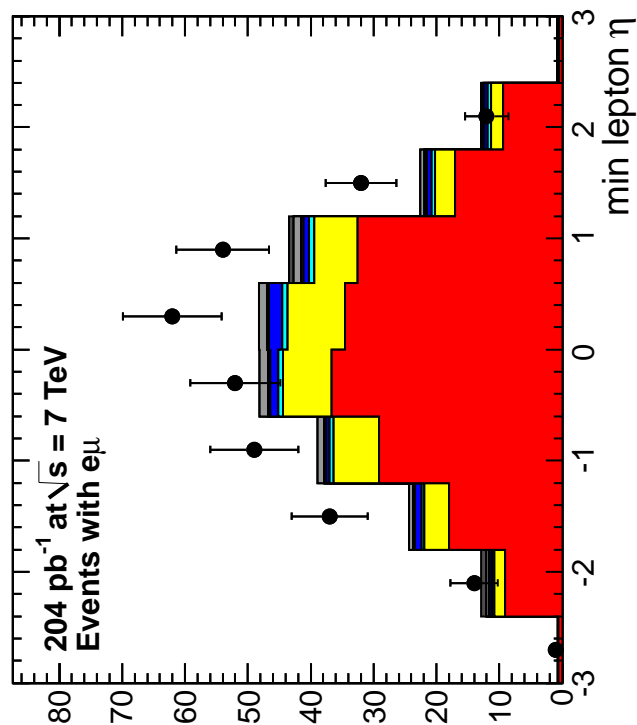
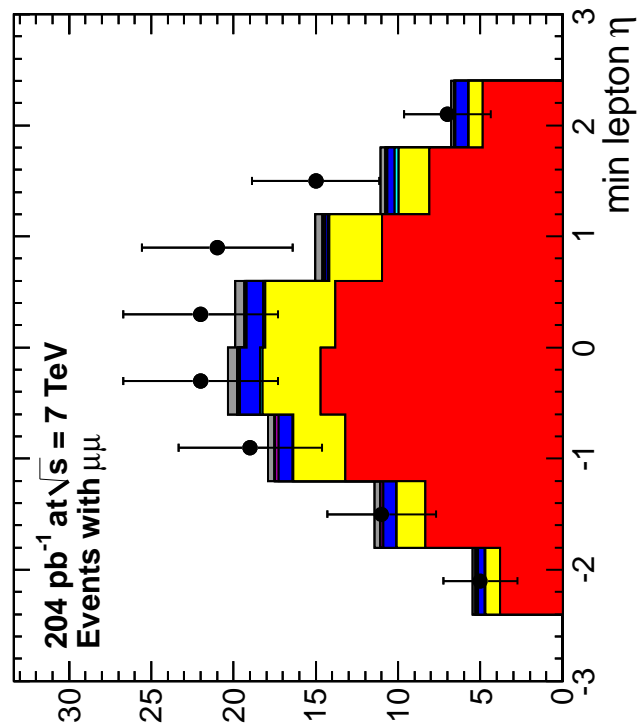
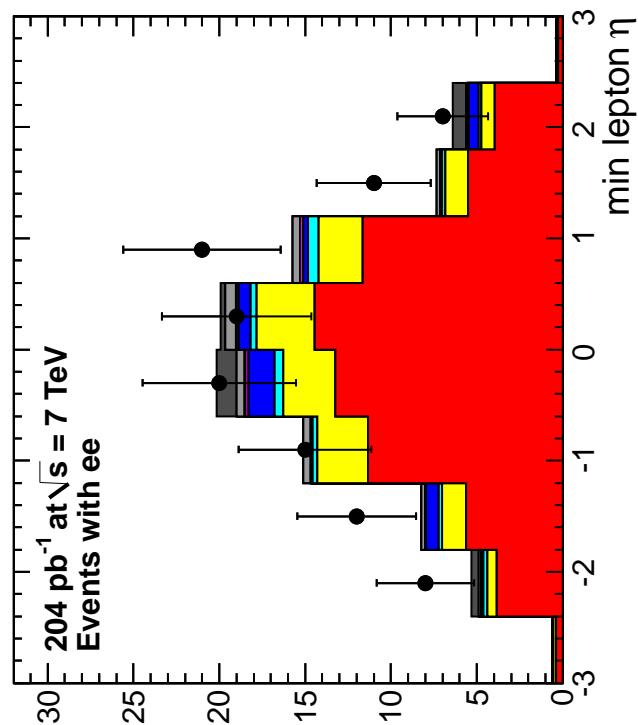
The meaning of most of the variables plotted in the following figures should be obvious. There are some exceptions that we explain below:

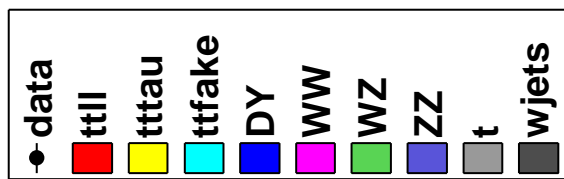
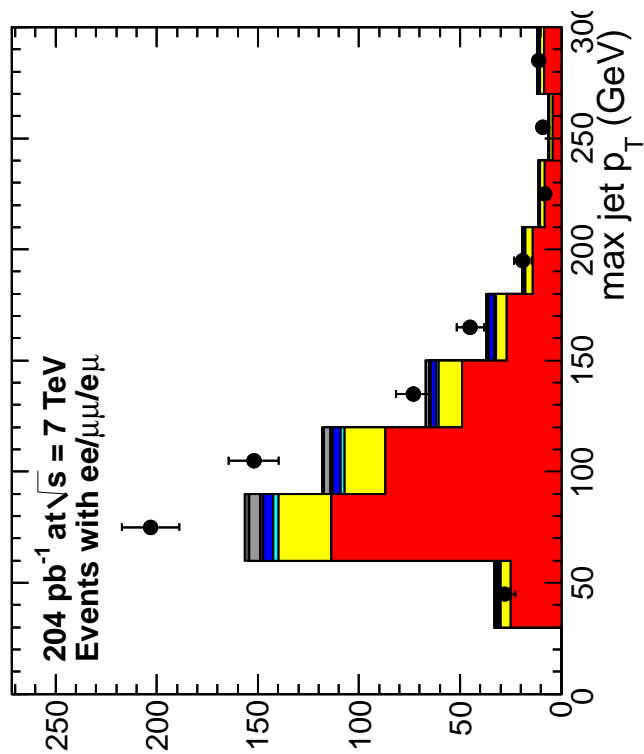
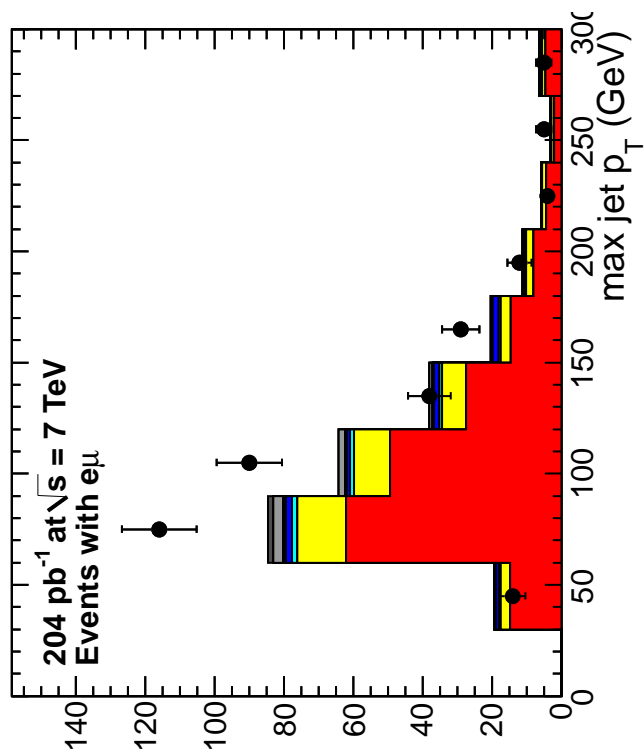
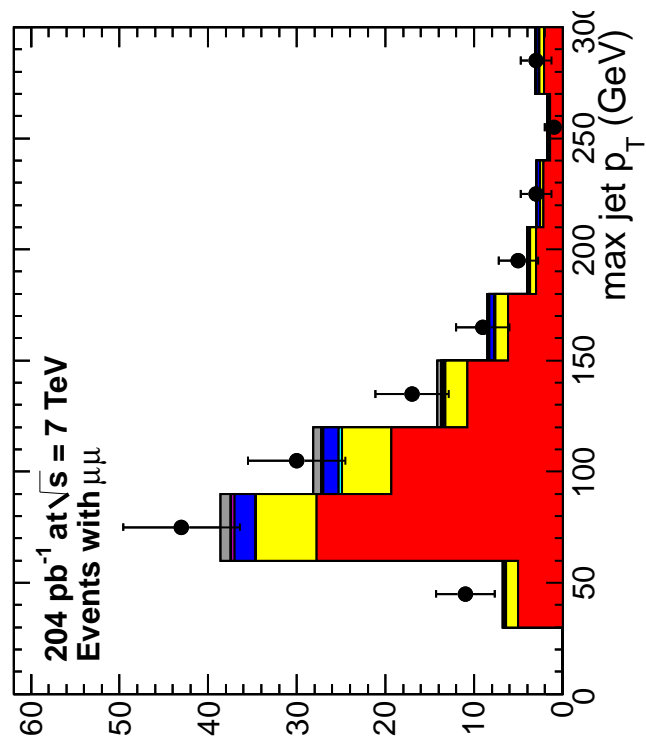
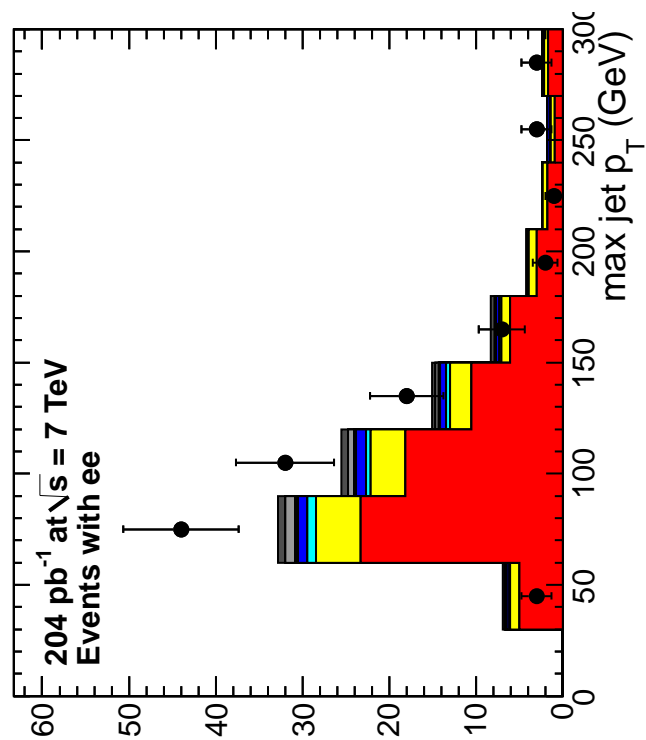
- $MT2$ is a kinematical quantity built from the two leptons and the E_T^{miss} . For events with two $W \rightarrow \ell$ decays it should have a sharp kinematical cutoff at W mass. For more details, see Reference [22].
- $MT2J$ is very much like $MT2$ but it is built out of the leptons, the E_T^{miss} and the two jets. For $t\bar{t}$ events it has a kinematical cutoff at M_{top} , with tails due to the fact that occasionally one of the b -jets is not found and is replaced by a gluon jet from ISR or FSR. For more details, see Reference [23].

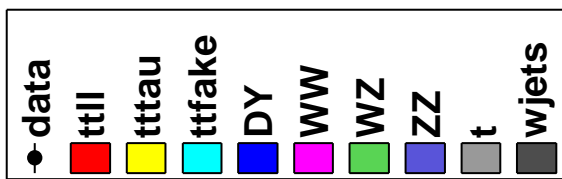
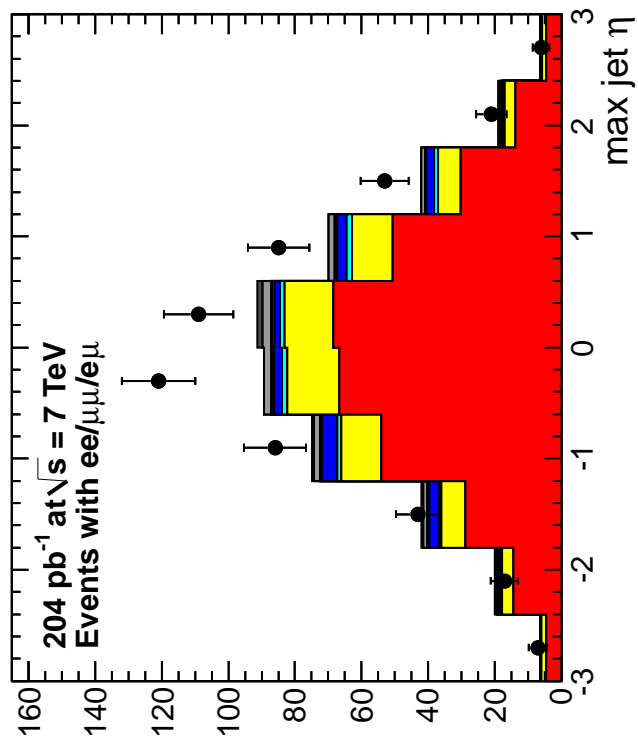
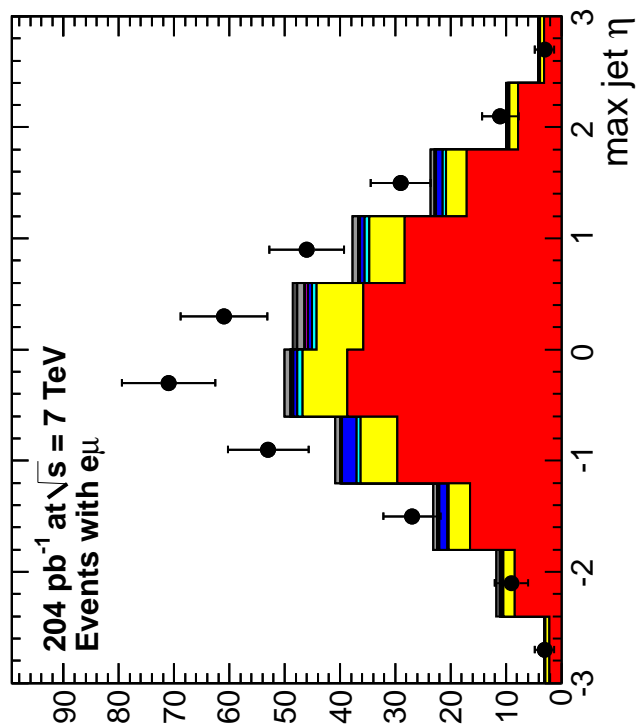
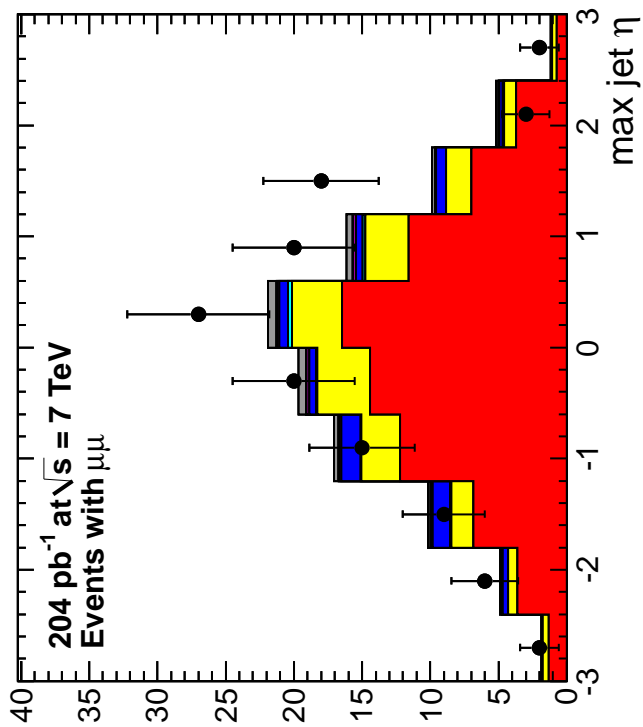
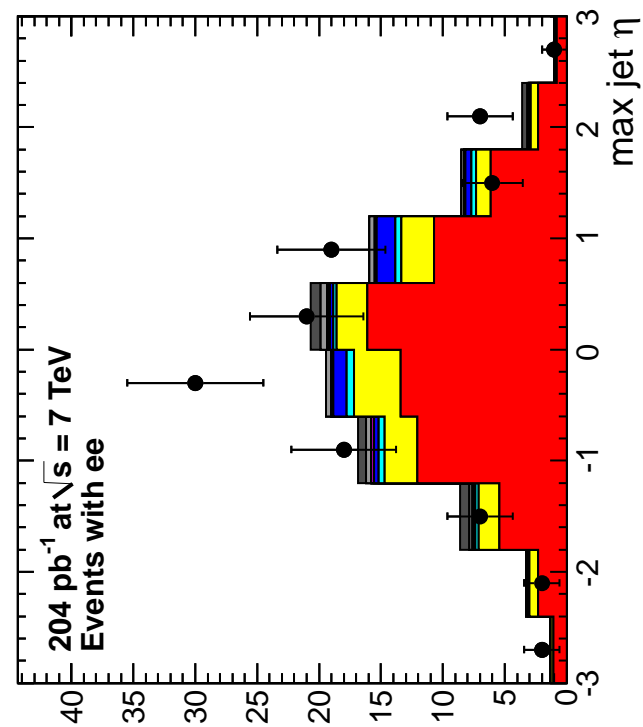


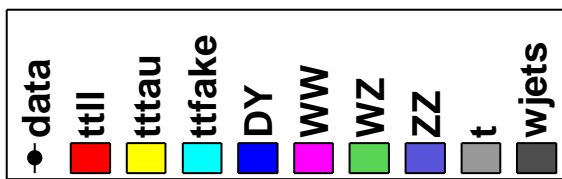
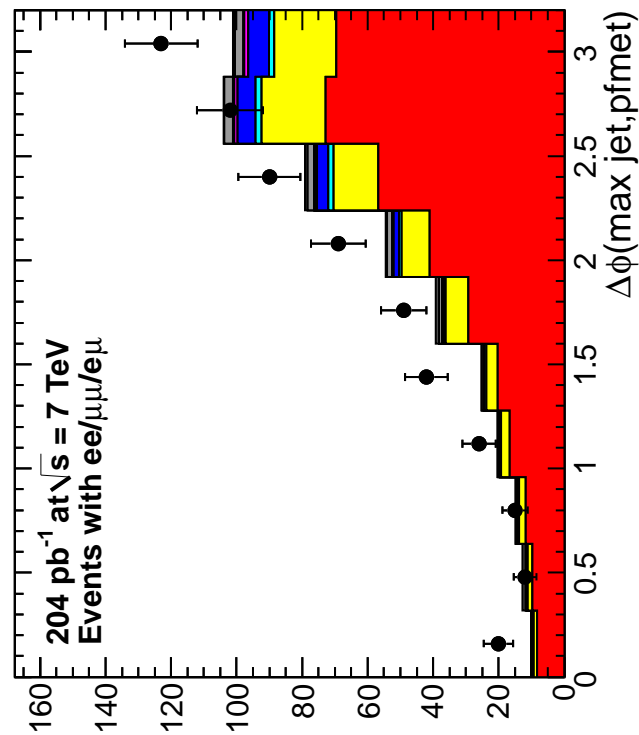
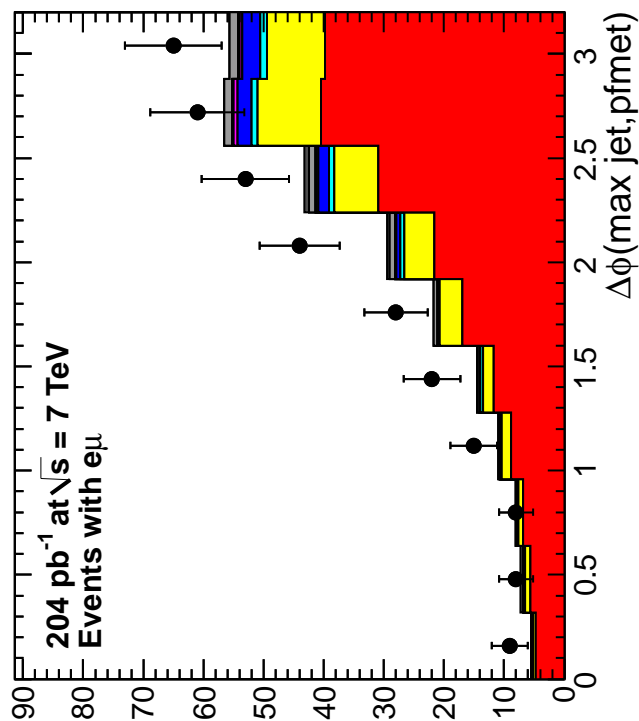
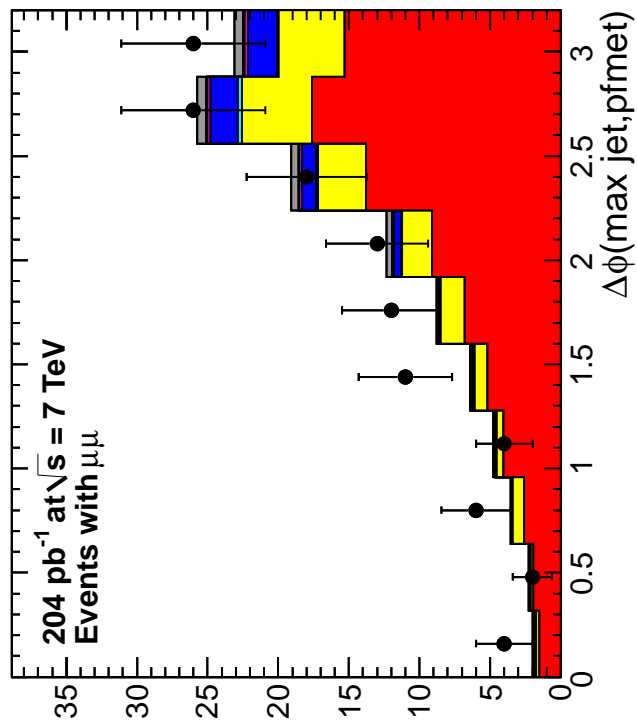
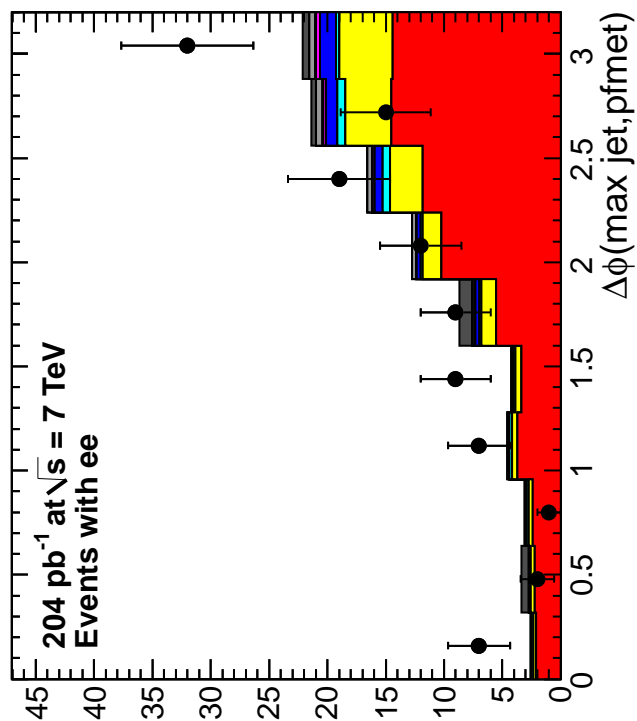


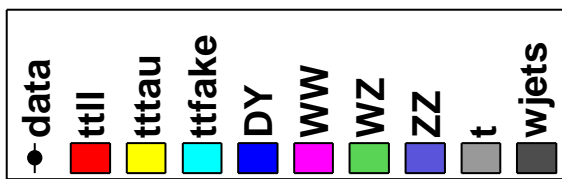
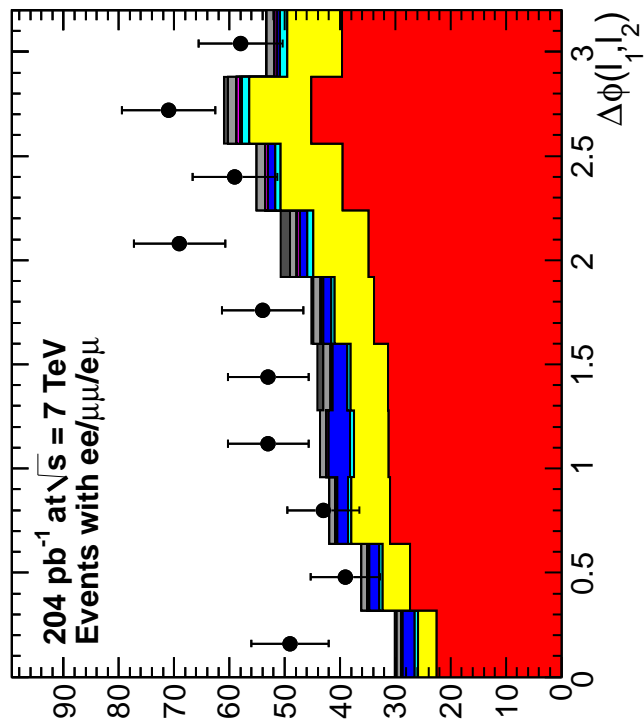
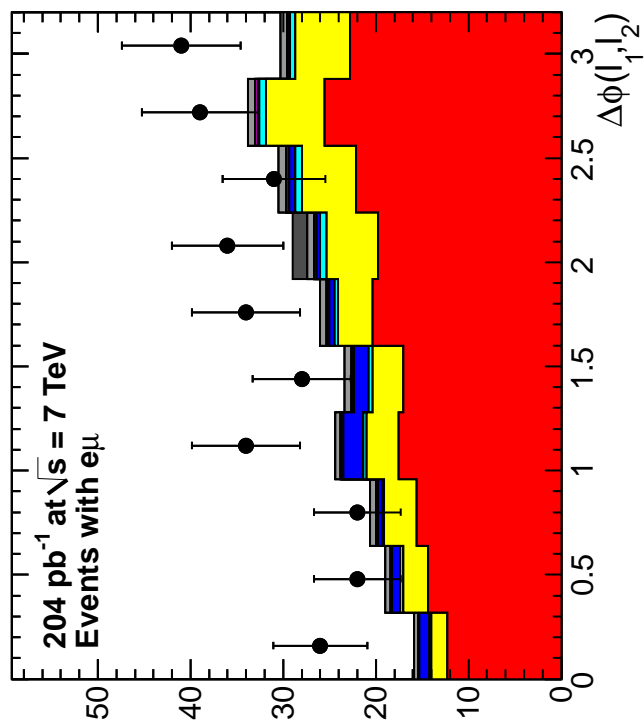
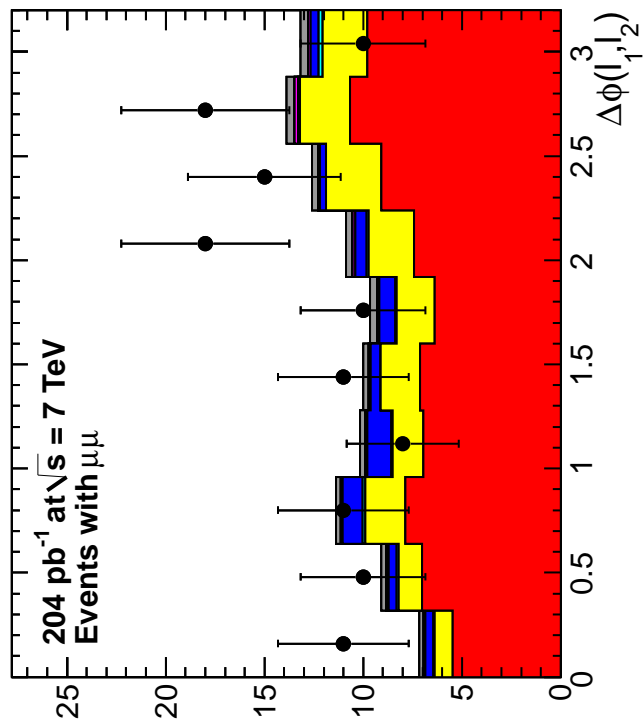
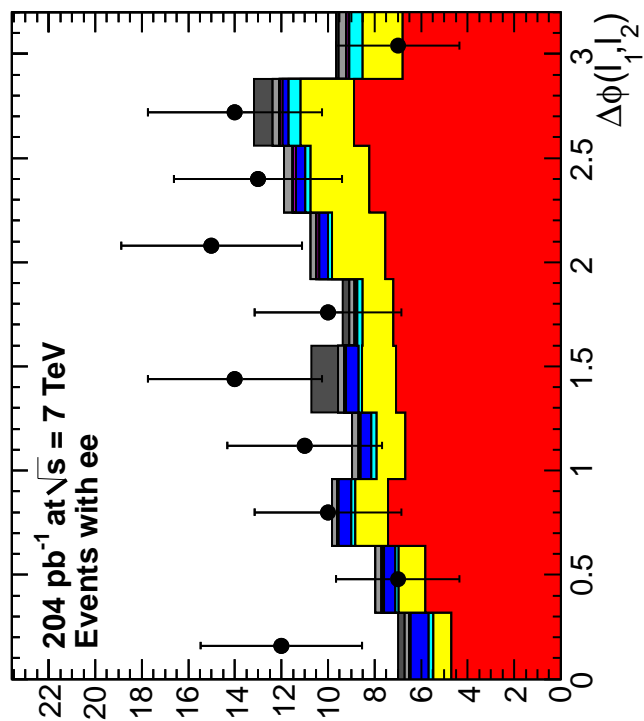


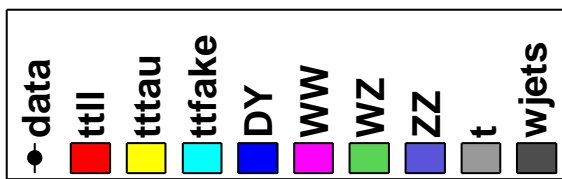
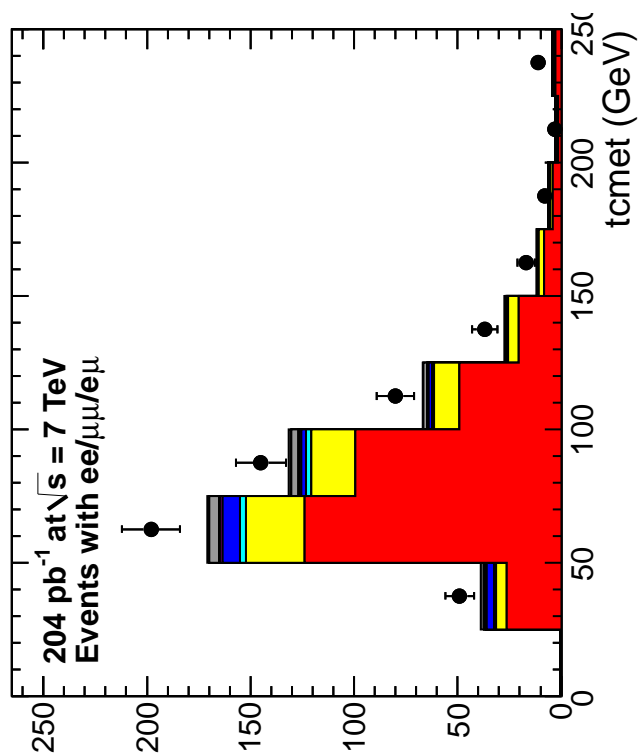
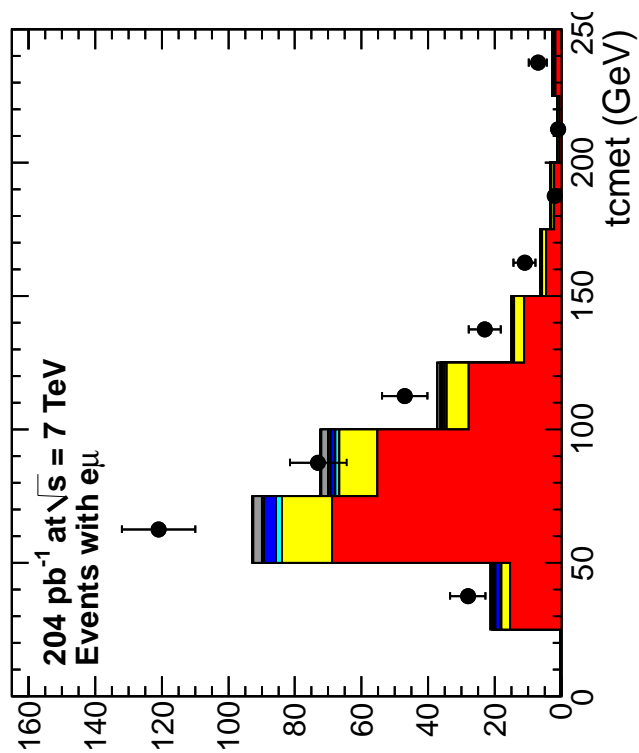
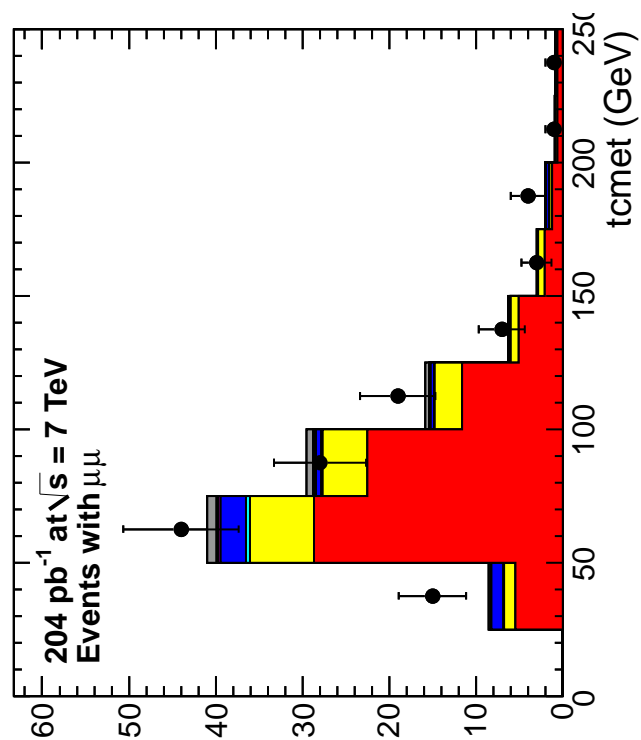
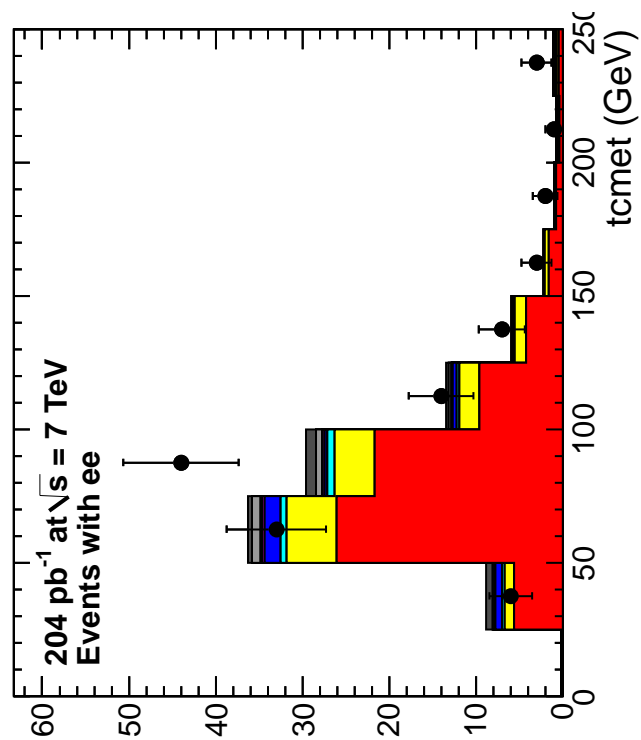


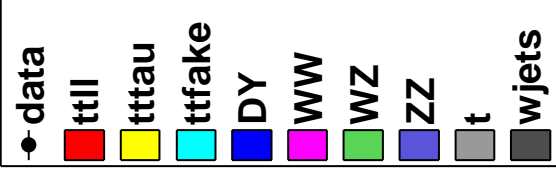
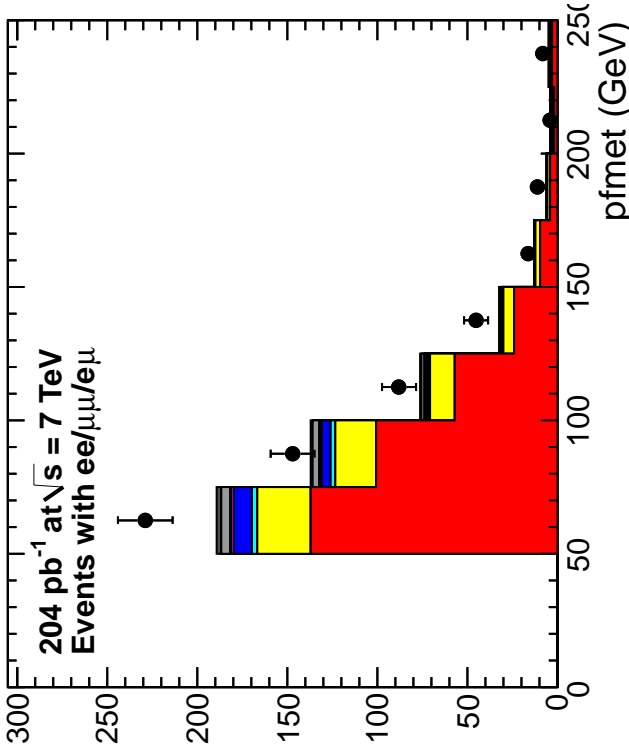
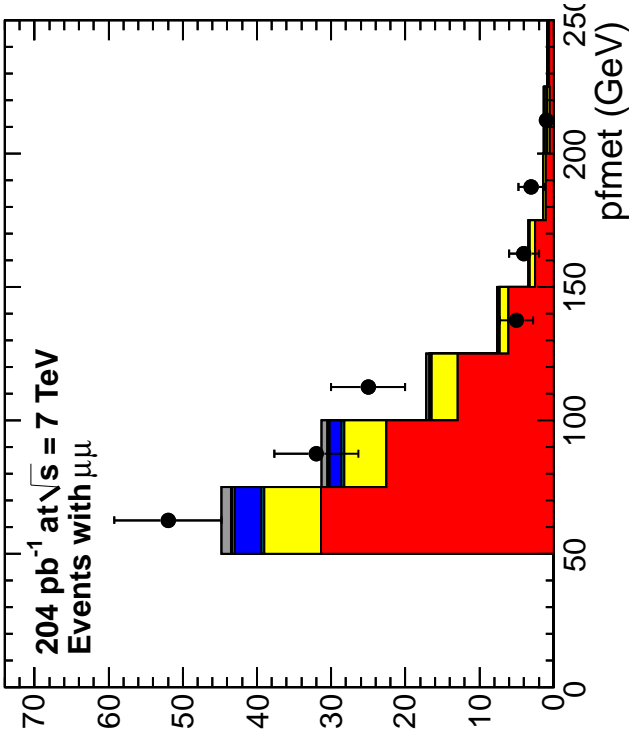
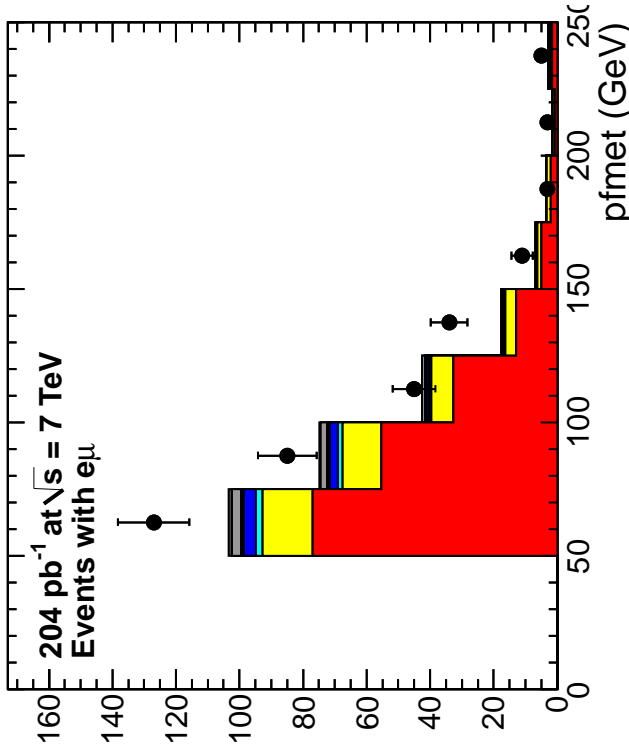
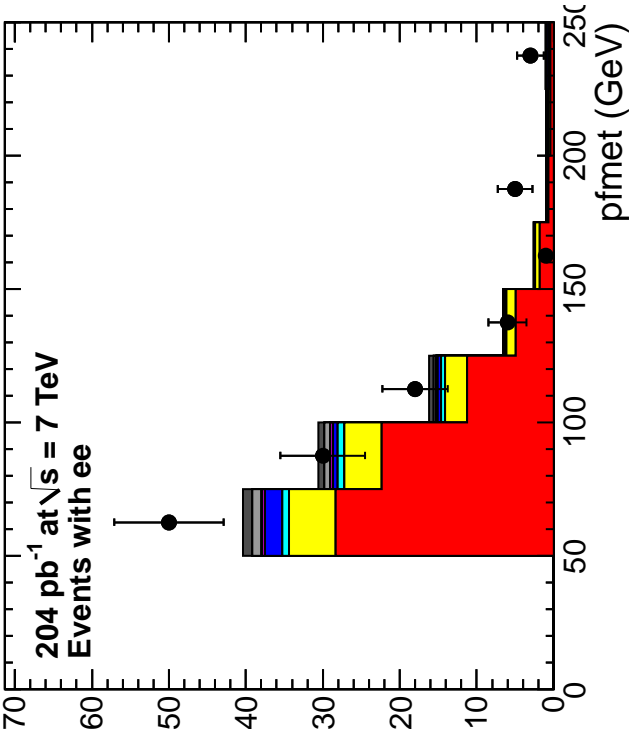


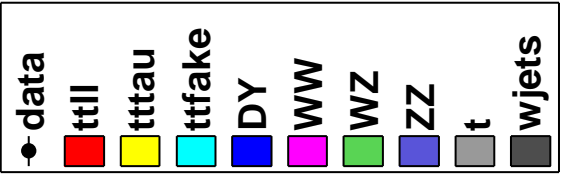
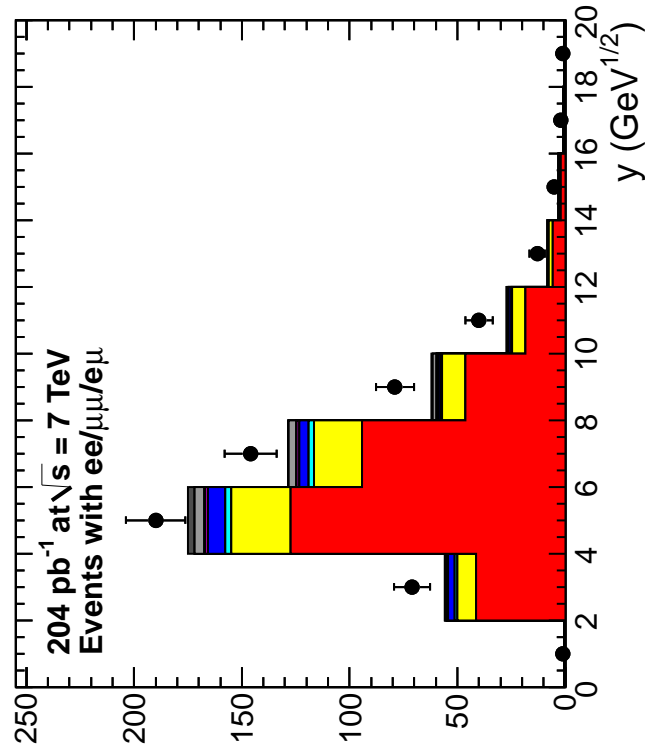
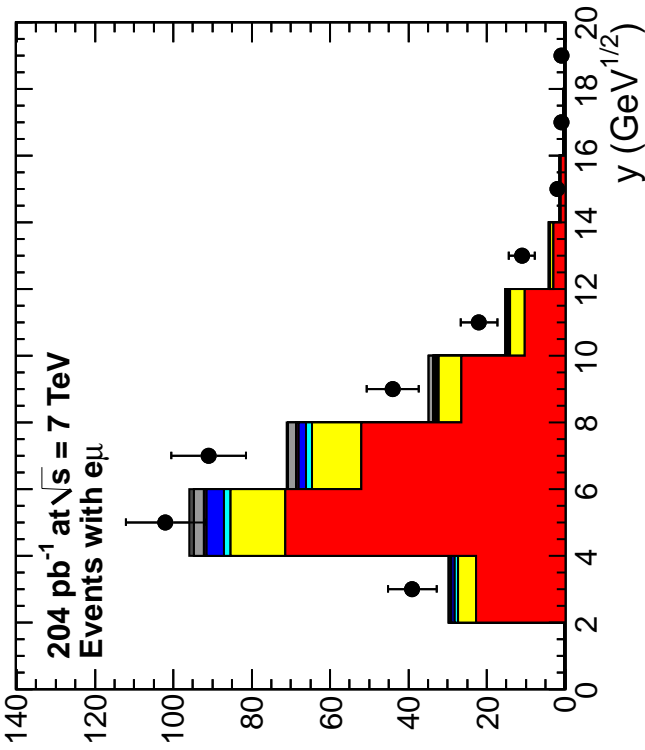
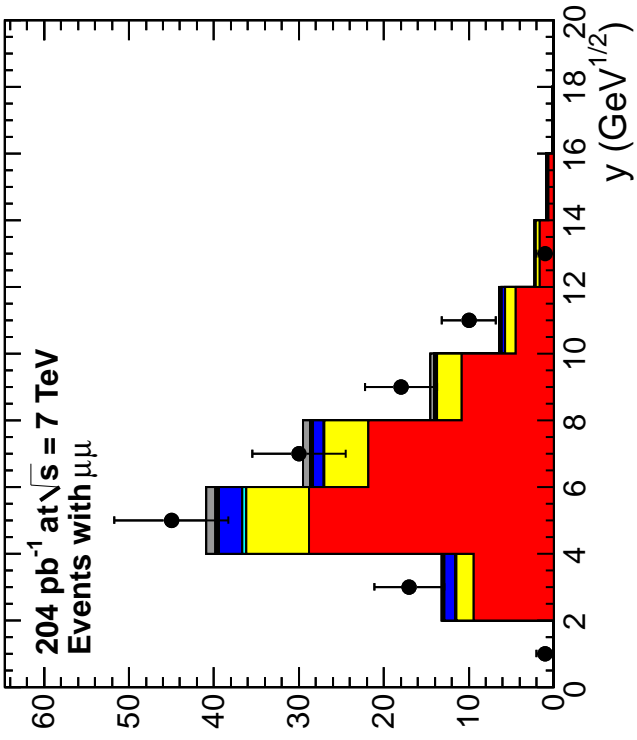
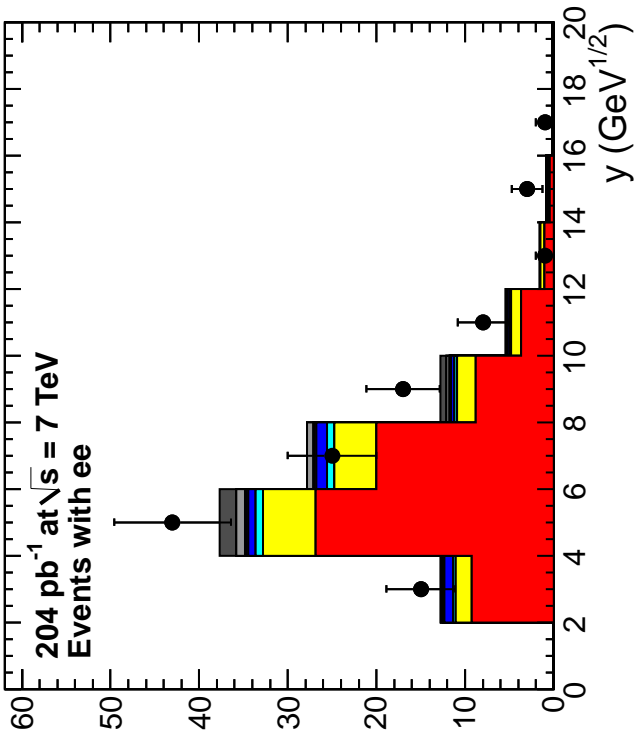


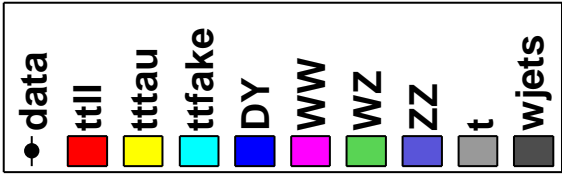
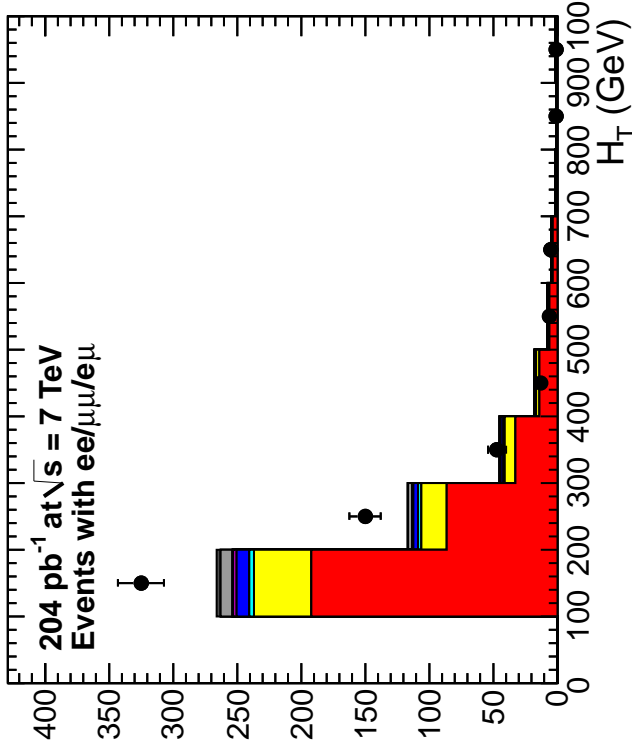
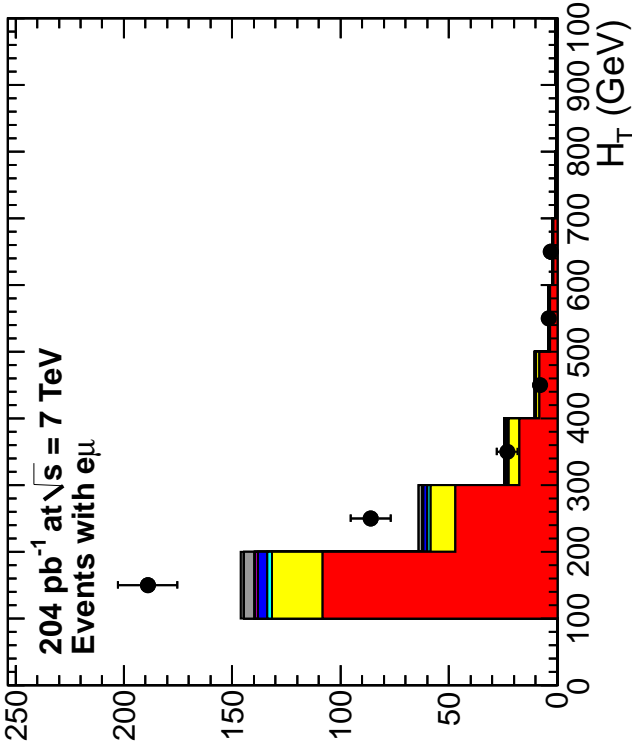
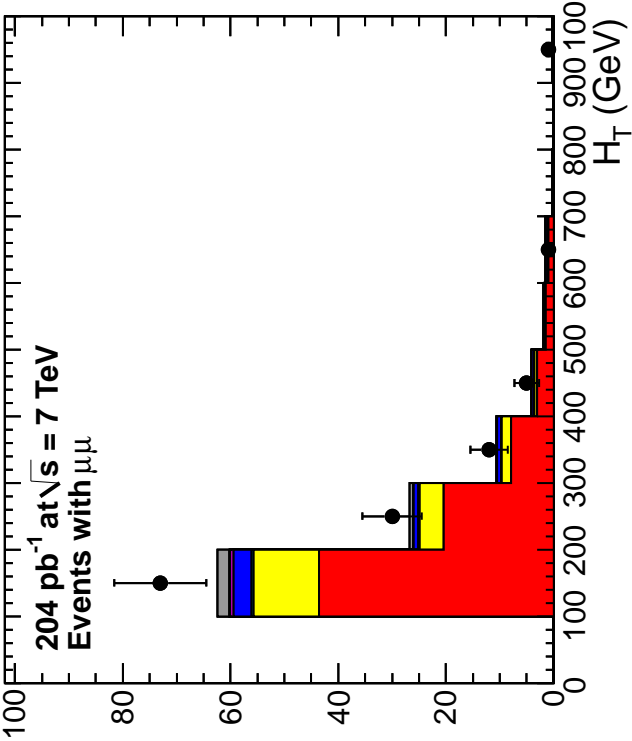
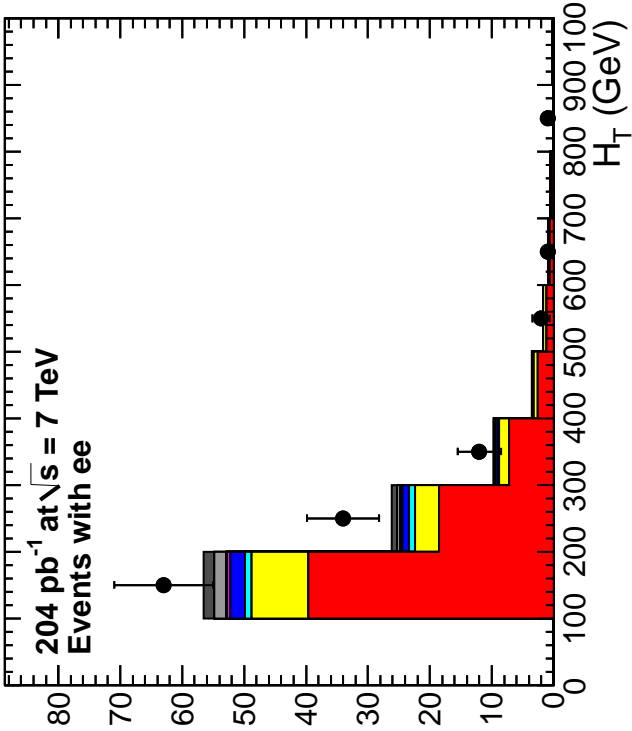


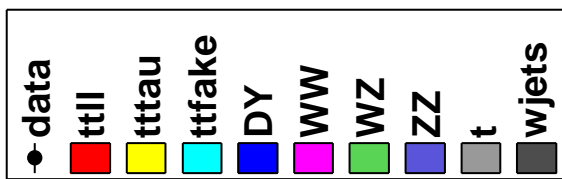
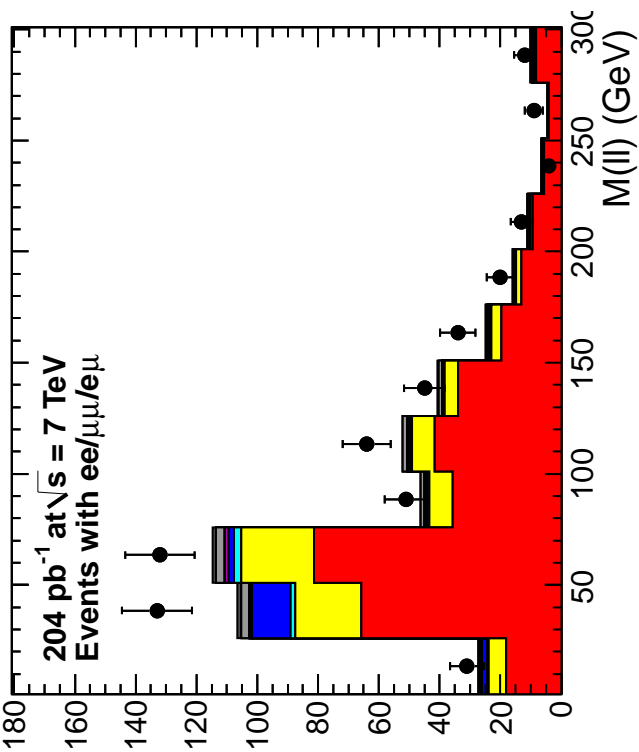
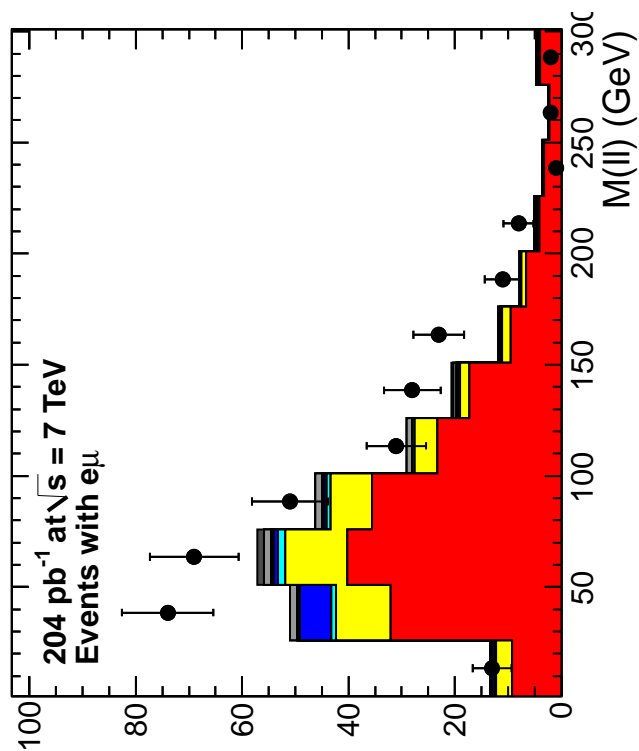
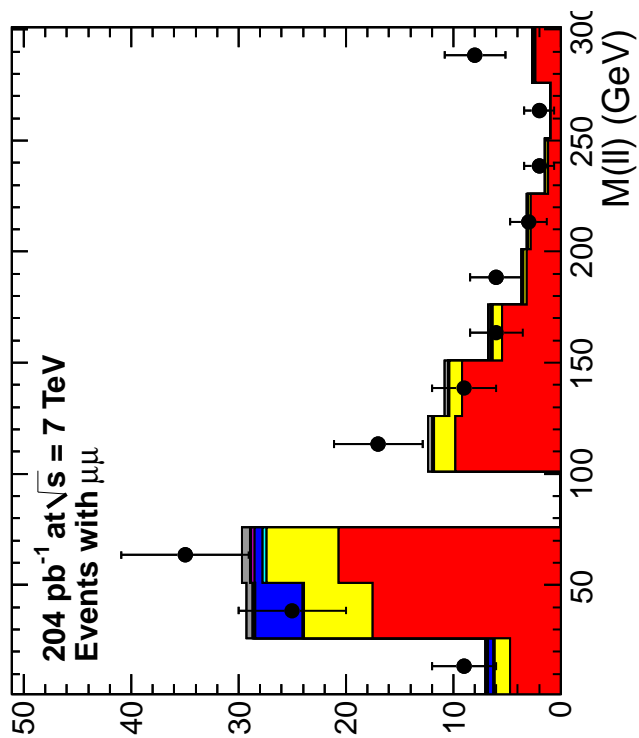
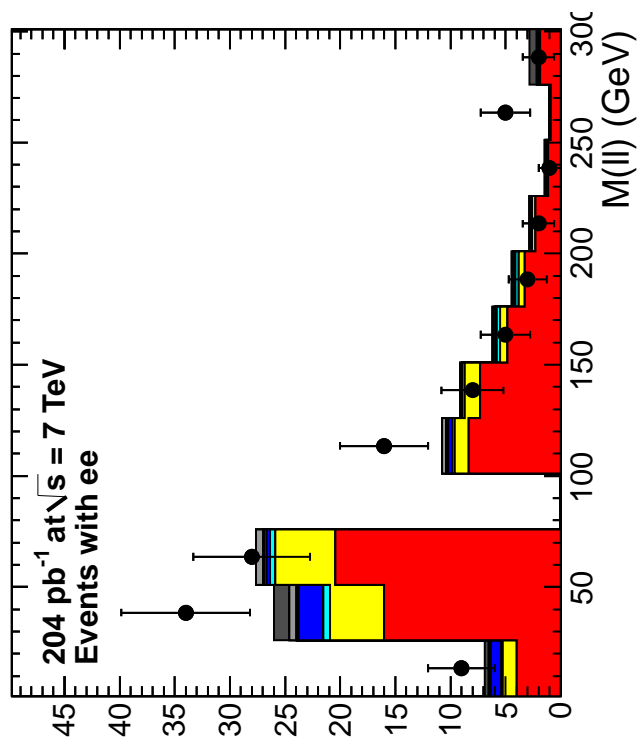


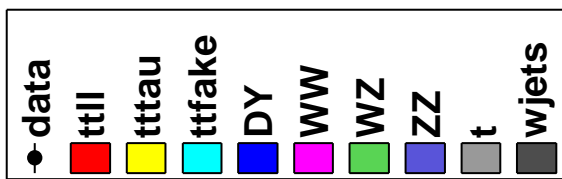
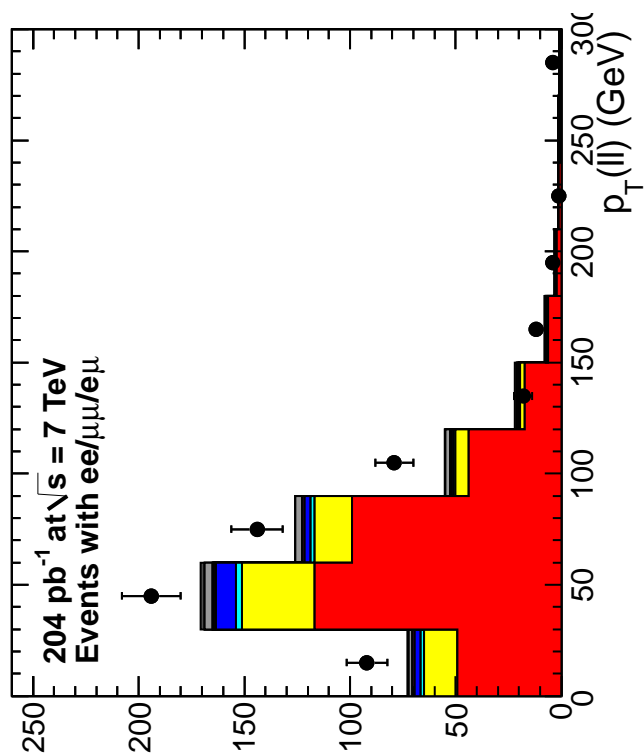
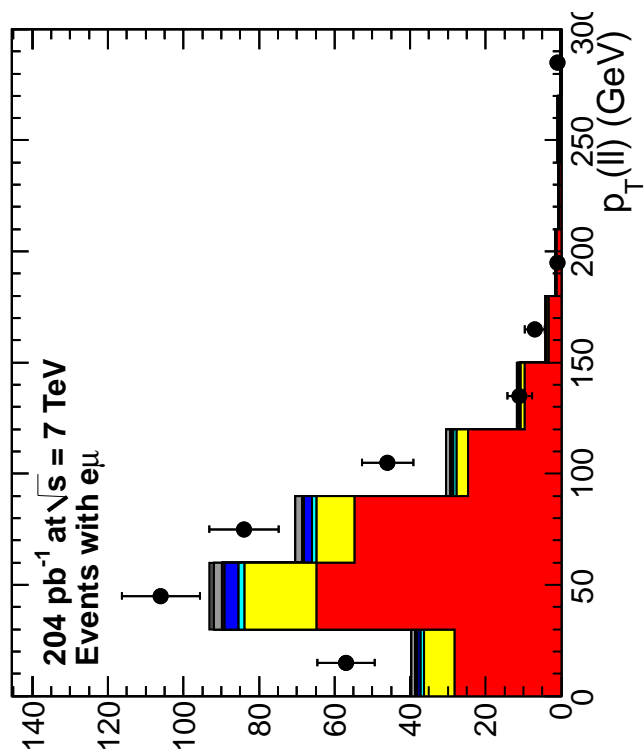
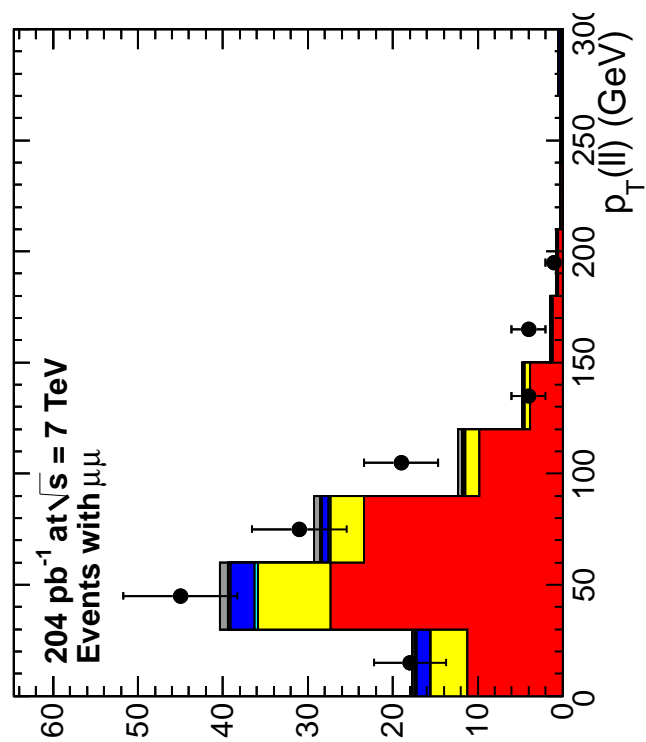
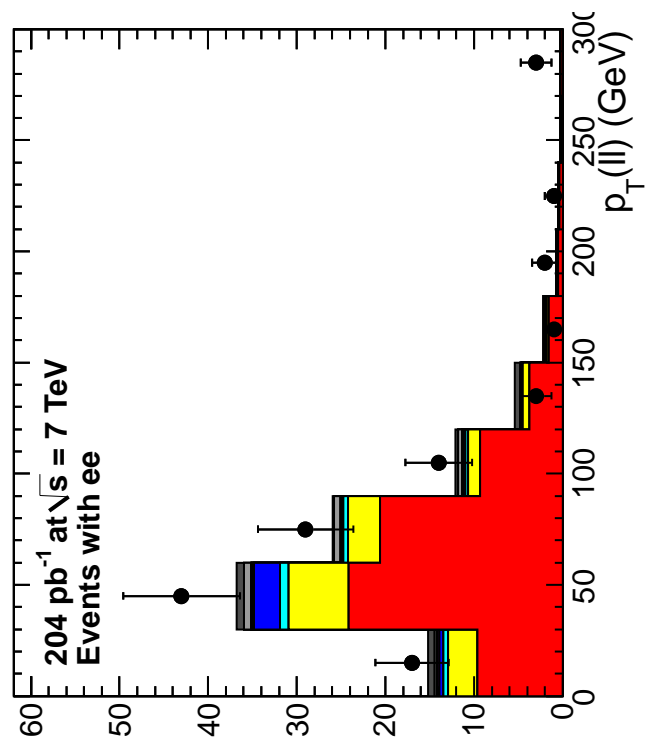


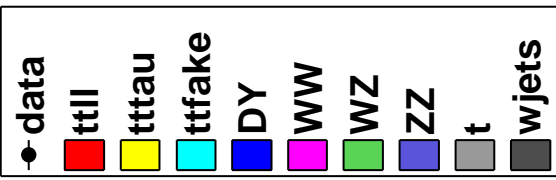
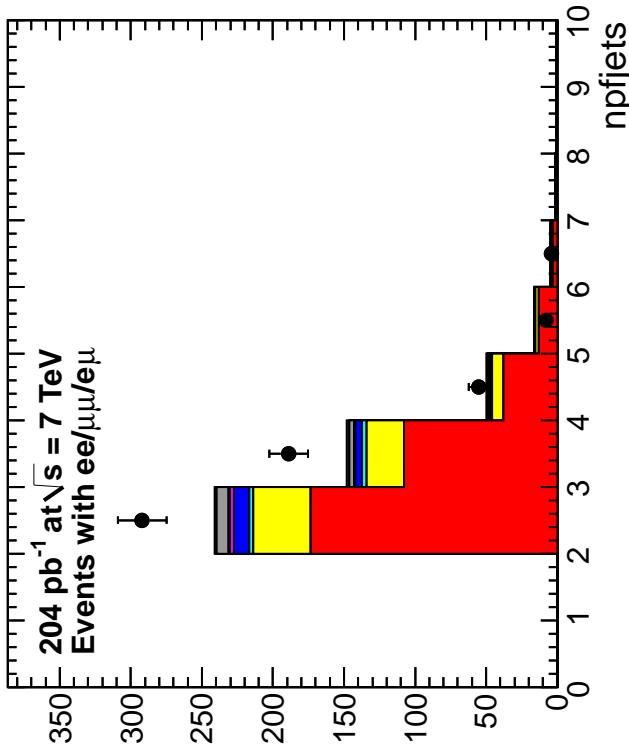
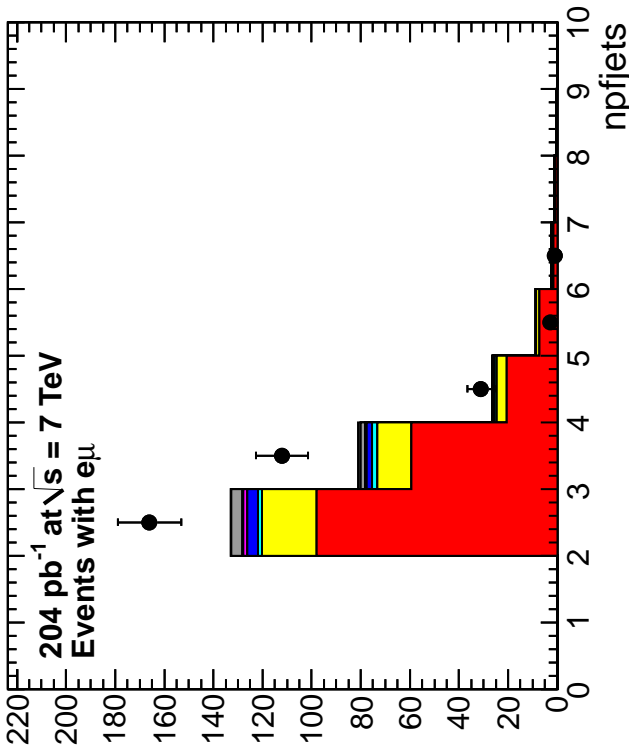
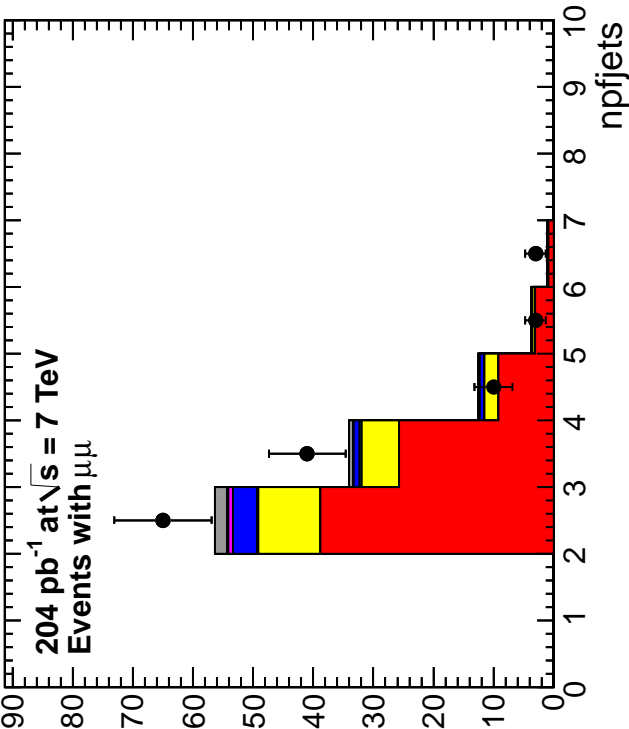
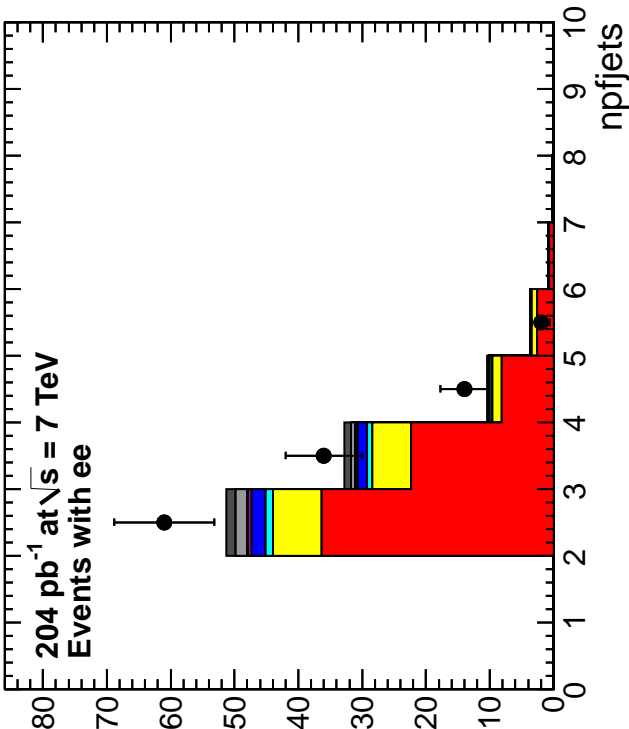


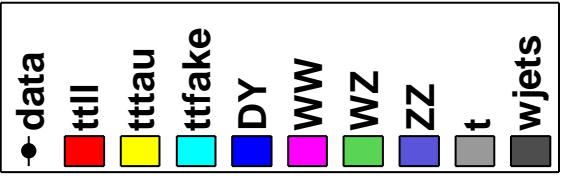
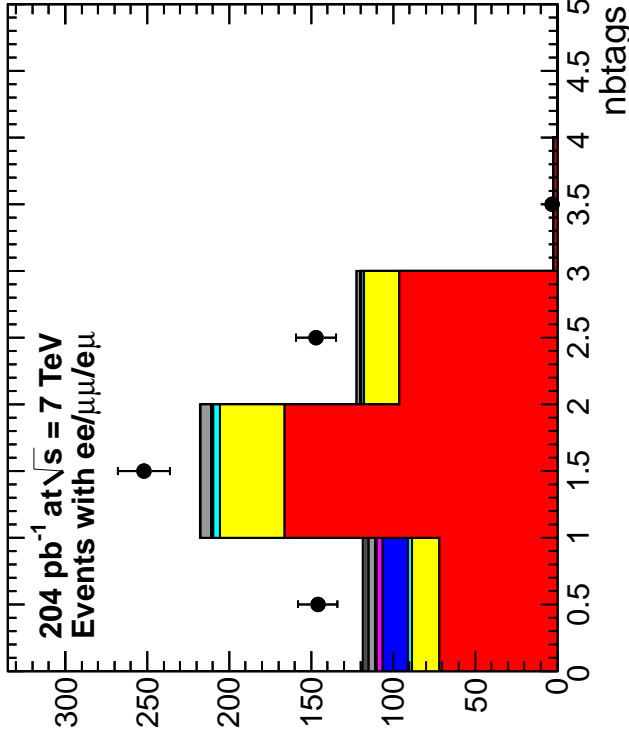
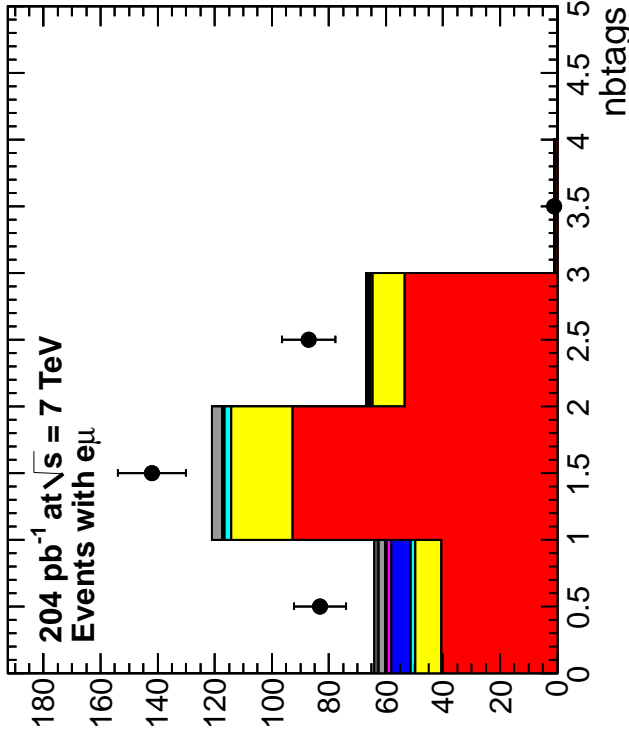
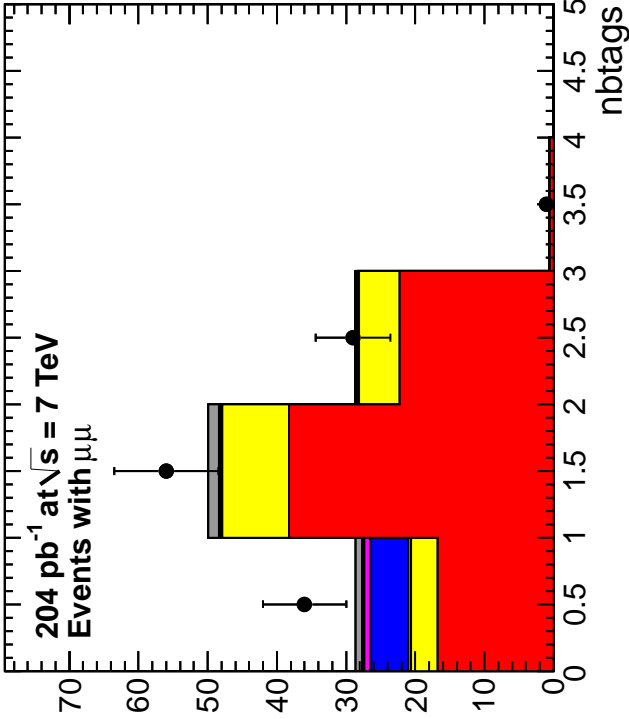
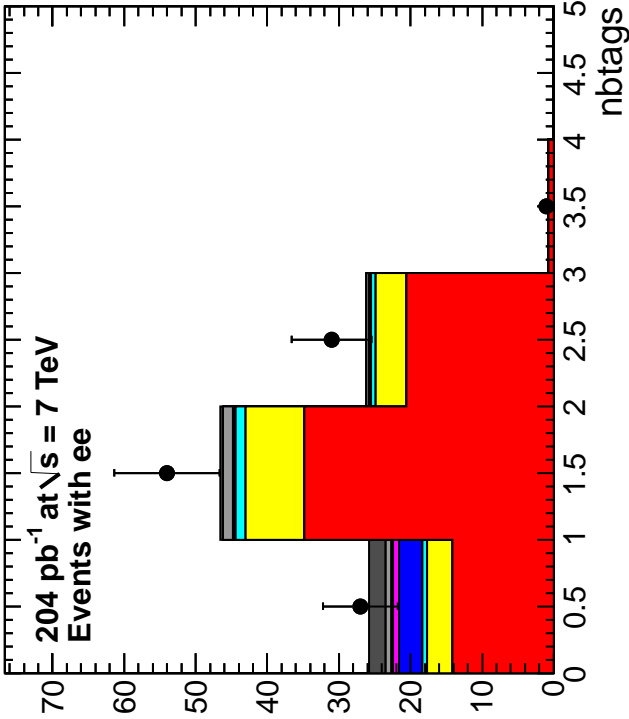


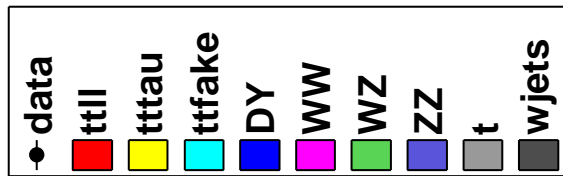
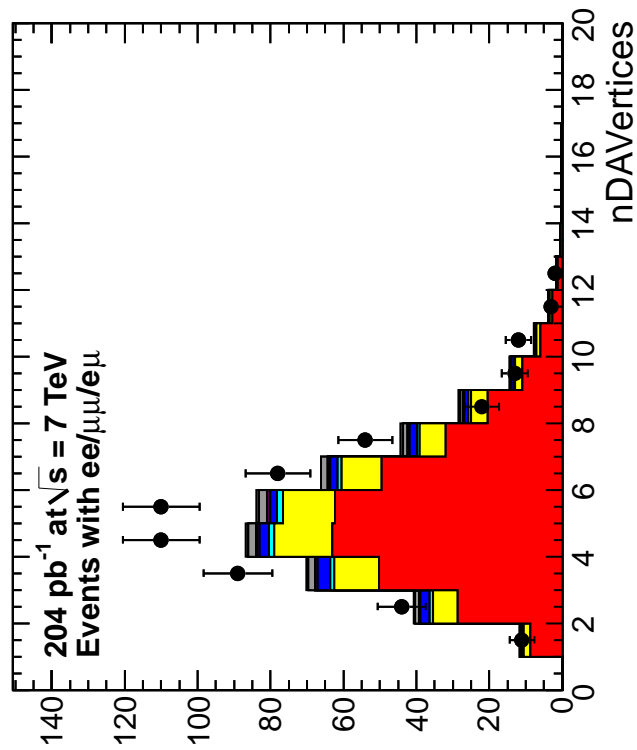
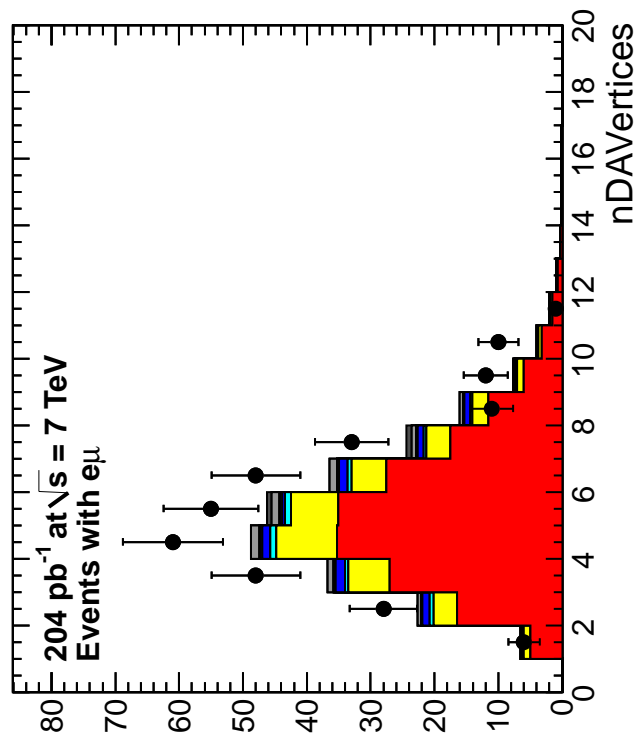
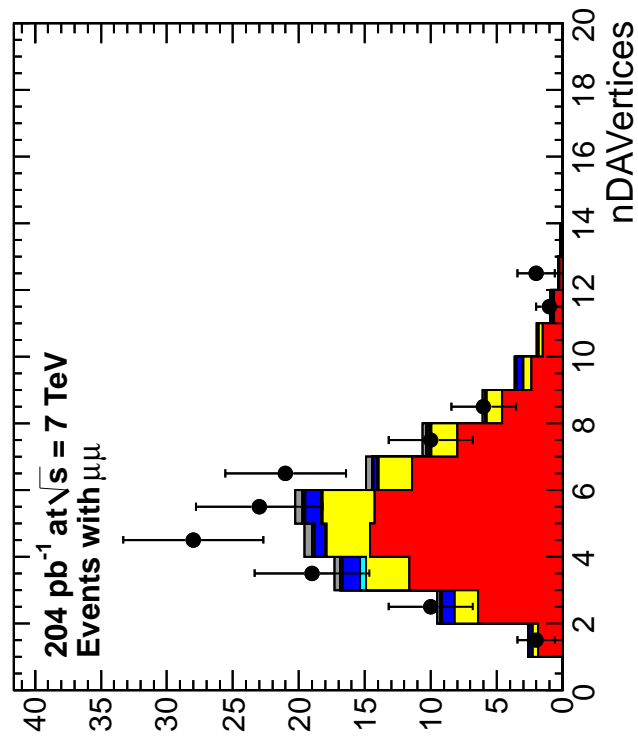
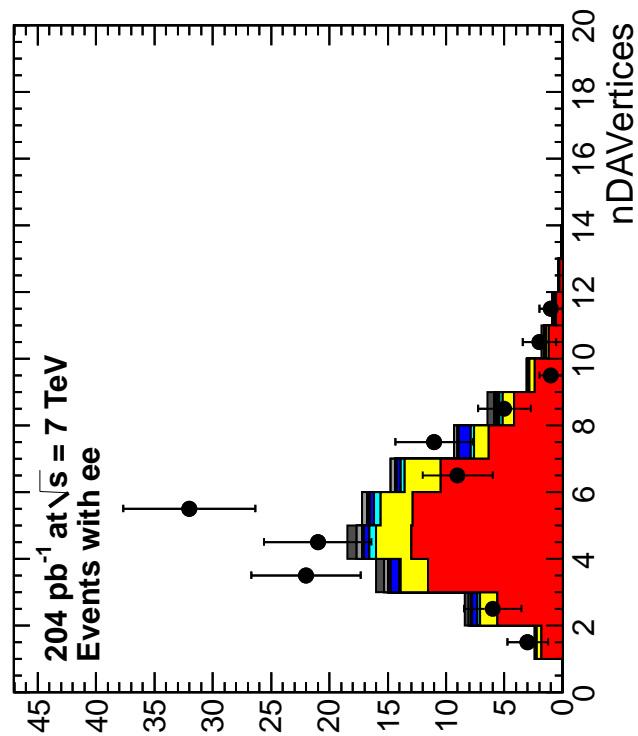


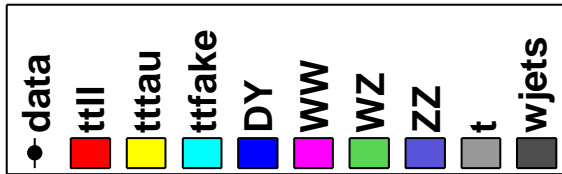
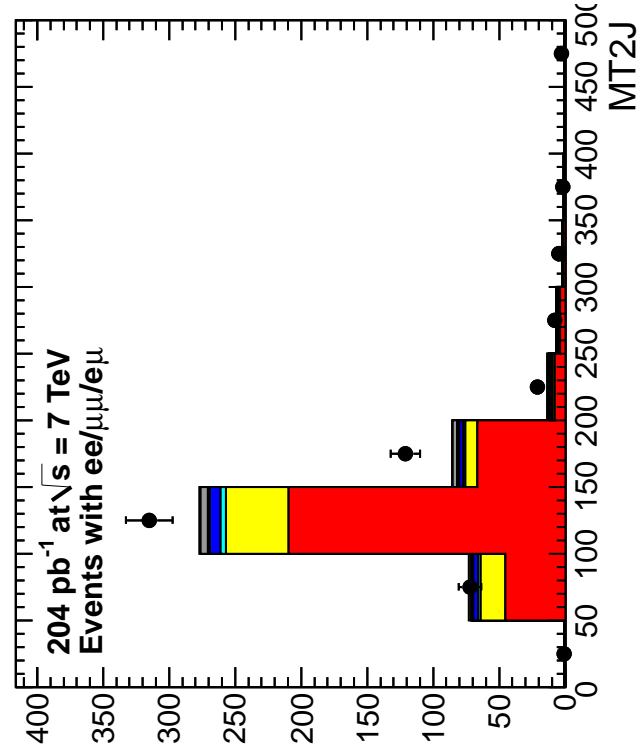
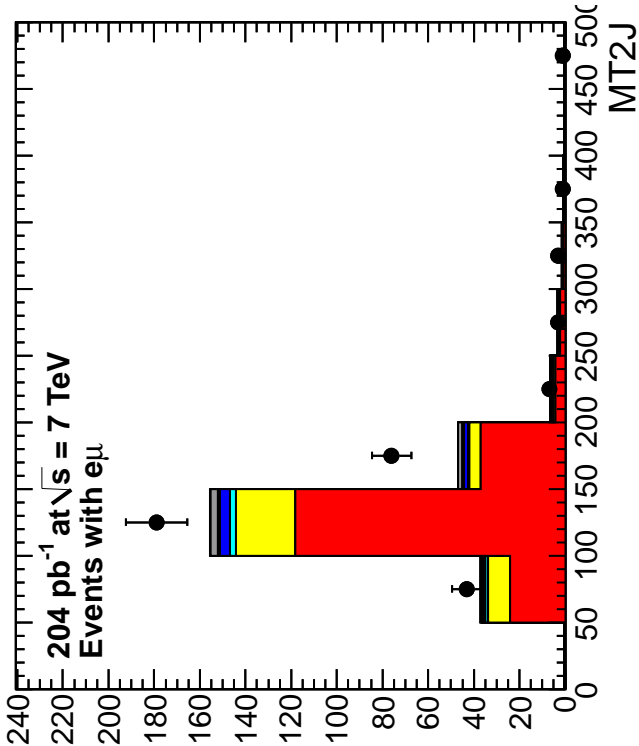
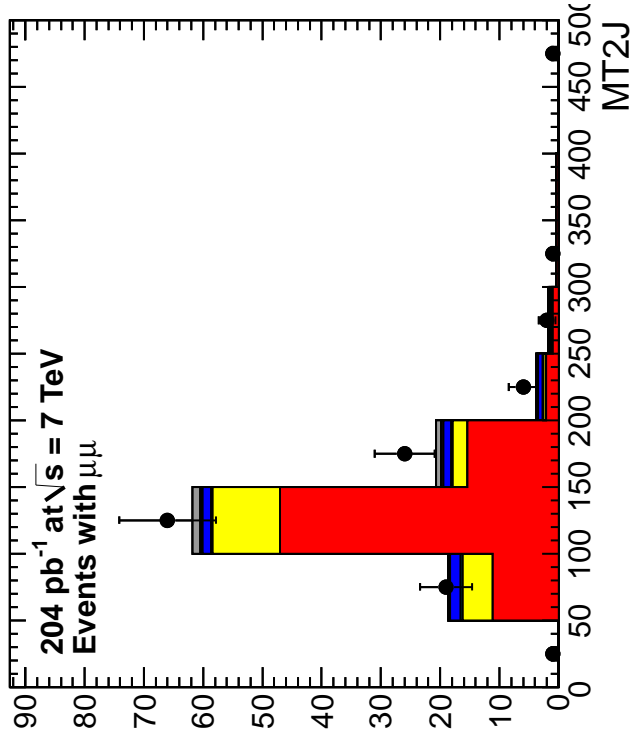
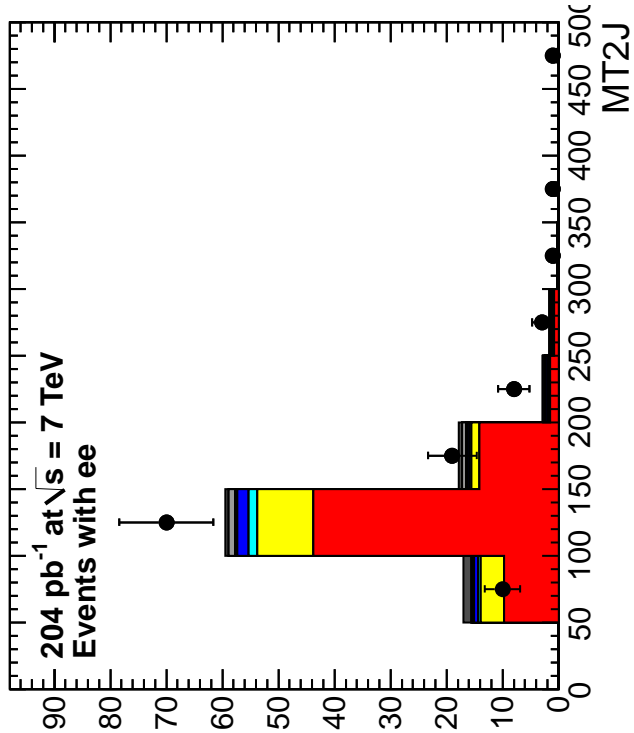


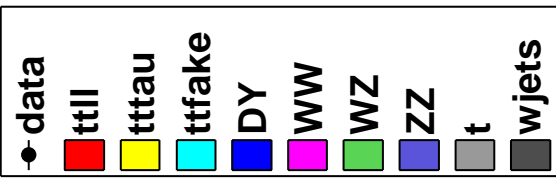
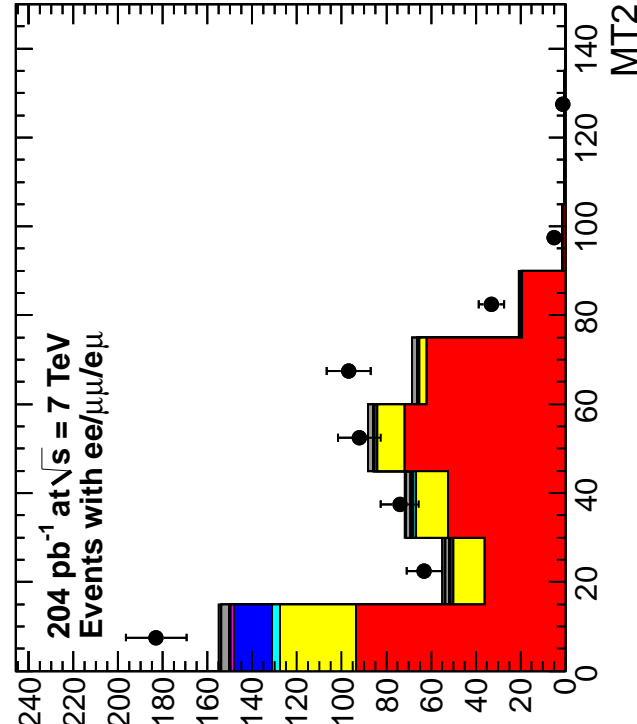
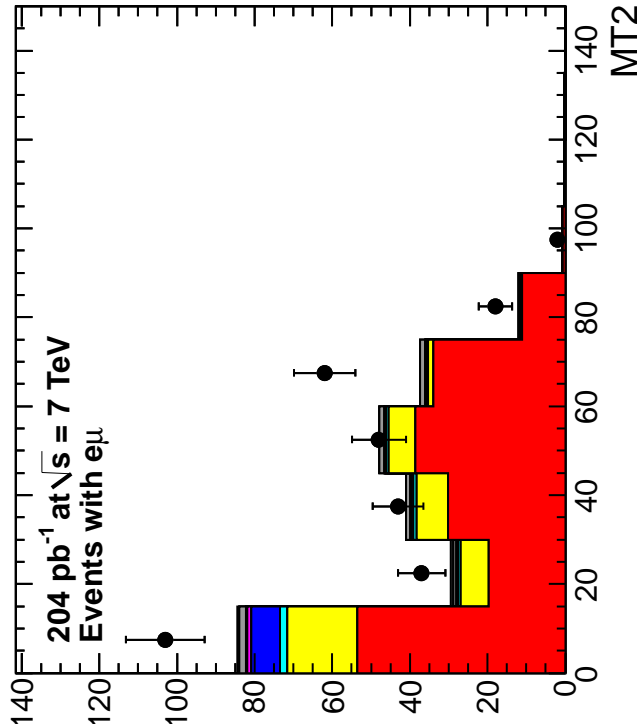
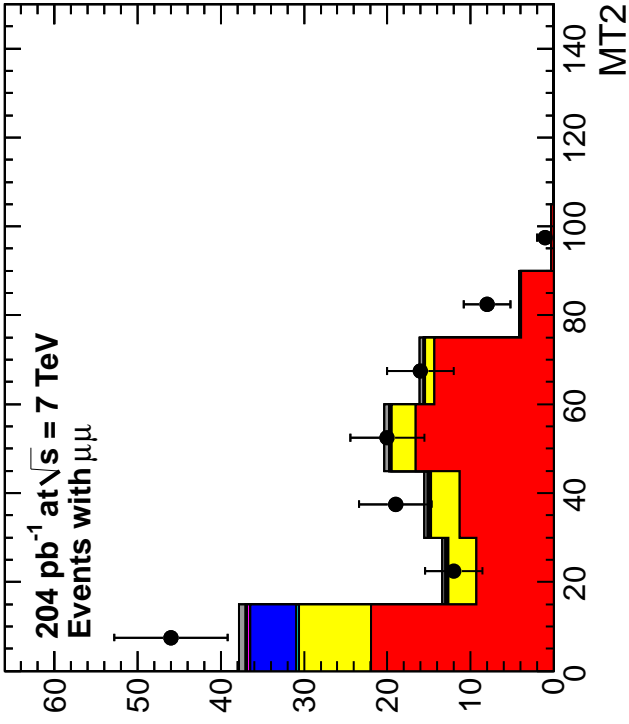
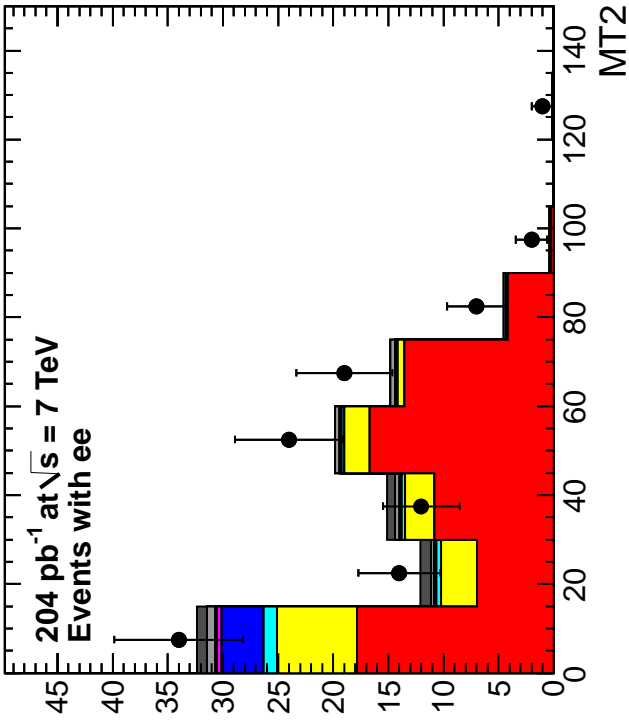


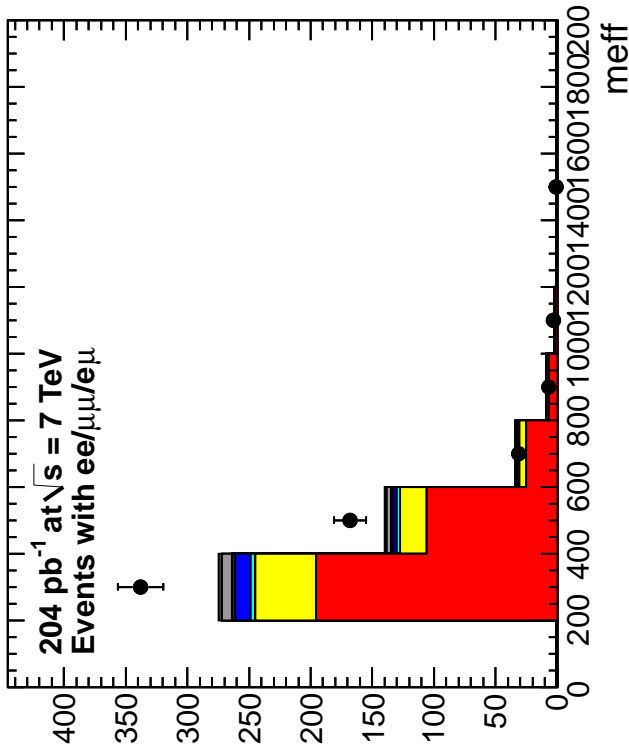
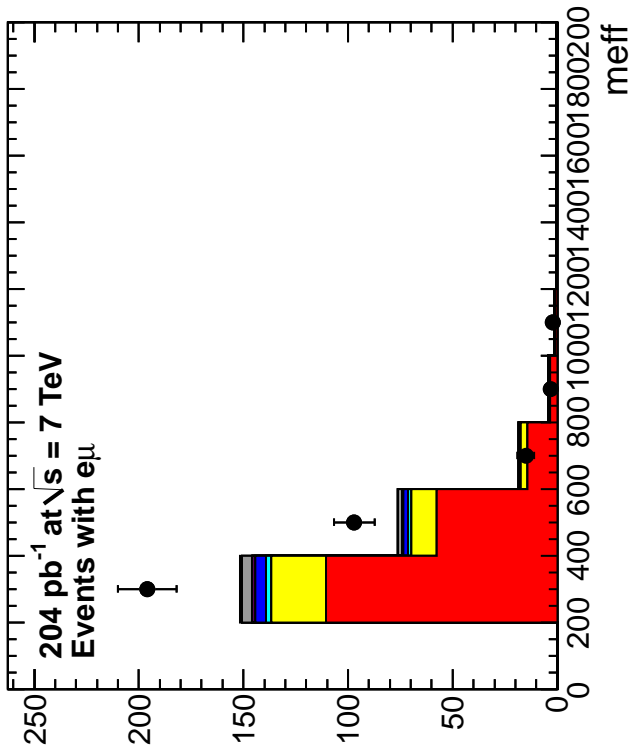
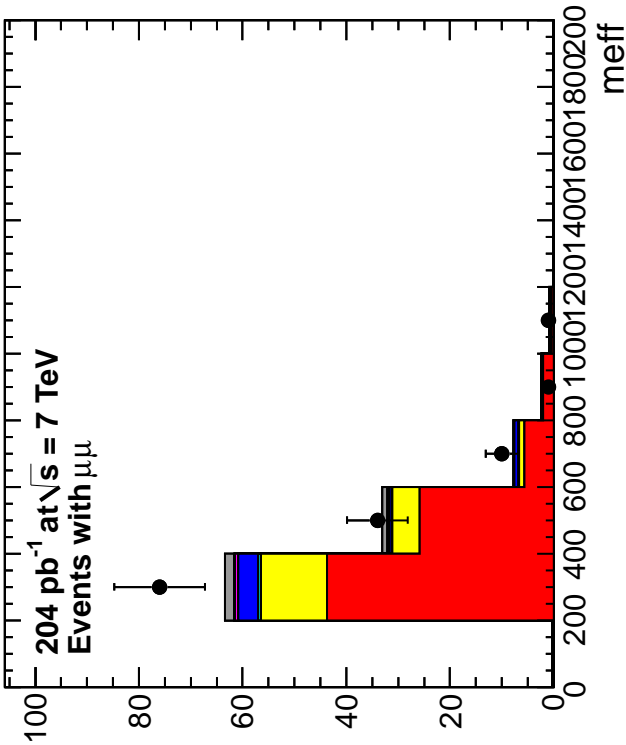
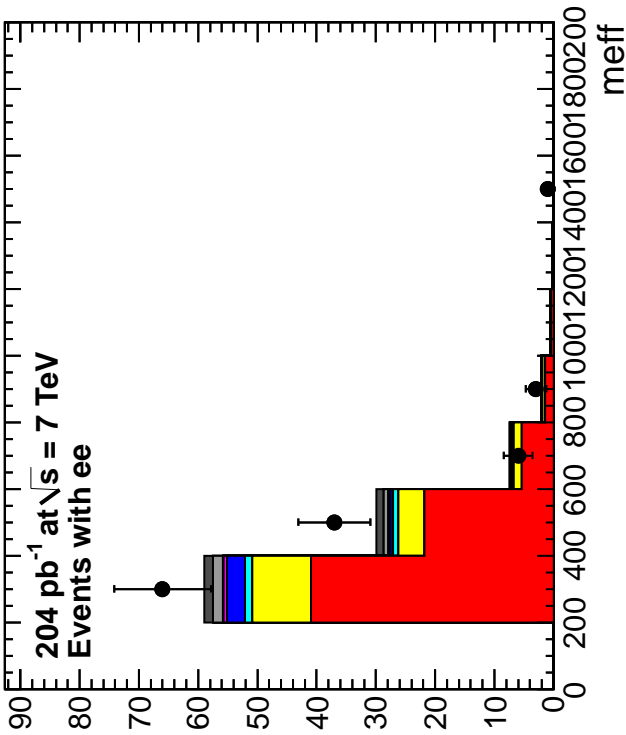












Appendix D Data/MC Comparison: 2010 Signal Region

Here we compare data and MC distributions for data passing the 2010 signal region requirements (preselection + $y > 8.5 \text{ GeV}^{1/2} + H_T > 300 \text{ GeV}$. The high p_T dilepton trigger data is used. We observe 14 events in this region.

